

California State University, San Bernardino

**CSUSB ScholarWorks**

---

Theses Digitization Project

John M. Pfau Library

---

2013

## Comparison and evaluation of black carbon and elemental carbon instrumentation in a near roadway environment

Brandon James Feenstra

Follow this and additional works at: <https://scholarworks.lib.csusb.edu/etd-project>



Part of the [Environmental Monitoring Commons](#)

---

### Recommended Citation

Feenstra, Brandon James, "Comparison and evaluation of black carbon and elemental carbon instrumentation in a near roadway environment" (2013). *Theses Digitization Project*. 4199.  
<https://scholarworks.lib.csusb.edu/etd-project/4199>

This Project is brought to you for free and open access by the John M. Pfau Library at CSUSB ScholarWorks. It has been accepted for inclusion in Theses Digitization Project by an authorized administrator of CSUSB ScholarWorks. For more information, please contact [scholarworks@csusb.edu](mailto:scholarworks@csusb.edu).

COMPARISON AND EVALUATION OF BLACK CARBON AND  
ELEMENTAL CARBON INSTRUMENTATION IN A NEAR  
ROADWAY ENVIRONMENT

---

A Project  
Presented to the  
Faculty of  
California State University,  
San Bernardino

---

In Partial Fulfillment  
of the Requirements for the Degree  
Master of Science  
in  
Earth and Environmental Sciences

---

by  
Brandon James Feenstra  
June 2013

COMPARISON AND EVALUATION OF BLACK CARBON AND  
ELEMENTAL CARBON INSTRUMENTATION IN A NEAR  
ROADWAY ENVIRONMENT

---

A Project  
Presented to the  
Faculty of  
California State University,  
San Bernardino

---

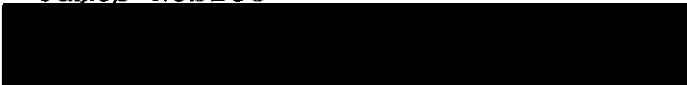
by  
Brandon James Feenstra

June 2013

Approved by:

  
Brett Stanley, Chair, Chemistry

  
James Noblet

  
Andrea Polidori

June 5, 2013  
Date

## ABSTRACT

The measurement of carbonaceous aerosol is a growing field of study because of increasing interest into the climate and health effects of black carbon (BC), an important constituent of atmospheric particulate matter (PM). Elemental carbon (EC) and BC are measurements of similar portions of carbon particulate matter, but the two measures are operationally defined according to the method used for their detection.

An instrument comparison study was conducted at a site adjacent to the I-710 freeway from March 7 to April 8 of 2012 to evaluate various BC and EC aerosol measurement methods. The list of BC and EC instruments includes seven continuous methods and two integrated filter methods. The photoacoustic extinctions, dual spot aethalometer, and micro aethalometers have not been compared in previous studies. Other continuous instruments include the multiple angle photometer, two aethalometers, and a semi-continuous carbon analyzer. The integrated filter methods included a transmissometer (BC) and a thermal-optical carbon analyzer (EC). The results of the comparison study show strong correlations ( $R^2 > 0.84$ ) for all the methods with a 24 hour averaging time. The slope values varied widely among the

methods with a range of 0.61 to 1.52. Overall, the results of the inter-comparison between all the instruments show strong correlations among the methods with wide slope variations. Strong correlations with slope variation indicate that differences are systematic and potentially reconcilable with the differences related to the assumptions and conversion factors used to estimate the concentration from an instrument signal.

## ACKNOWLEDGEMENTS

I would like to acknowledge those who contributed to this instrument comparison study. I would like to first thank my graduate advisory committee members including Dr. Brett Stanly (CSUSB), Dr. James Noblet (CSUSB), and Dr. Andrea Polidori (SCAQMD). Dr. Polidori has been an outstanding advisor for the field work, data analysis, and writing portion of this project. I would also like to thank Dr. Tony Hansen from Magee Scientific. Dr. Hansen visited the site on several occasions and assisted in the data analysis portion of the study. Thank you for your help and advice on all things related to BC.

I would also like to acknowledge the participating companies and universities involved. Thank you to the University of California, Riverside (UCR) for loaning and operating the MAAP instrument. Thank you to Droplet Measurement Technologies (DMT) for loaning and operating the PAX instrument. Thank you to the USEPA for loaning the Sunset semi-continuous carbon analyzer. Thank you to Magee Scientific for loaning the dual spot aethalometer.

I thank those individuals who were involved in the instrument comparison study. Daniel Short from UCR operated the MAAP. I thank Bob Cary from Sunset Laboratories for the

installing the semi-continuous carbon analyzer. Thanks to John Walker from Droplet Measurement Technologies for installing and remotely operating the PAX.

## TABLE OF CONTENTS

ABSTRACT . . . . .	iii
ACKNOWLEDGEMENTS . . . . .	v
LIST OF TABLES . . . . .	ix
LIST OF FIGURES . . . . .	x
CHAPTER ONE: INTRODUCTION	
Background . . . . .	1
Carbonaceous Particulate Matter . . . . .	3
Measurement Techniques . . . . .	11
Purpose and Objectives . . . . .	12
Scope and Significance . . . . .	12
Definitions of Terms . . . . .	13
CHAPTER TWO: LITERATURE REVIEW	
Comparisons among Continuous Methods . . . . .	18
Comparisons among Integrated Methods . . . . .	27
Comparisons between Integrated and Continuous Methods . . . . .	29
CHAPTER THREE: METHODOLOGY	
Site Description and Timing . . . . .	34
Instrumentation . . . . .	36
Statistical Analysis of the Data . . . . .	62
Quality Assurance and Quality Control . . . . .	63



CHAPTER FOUR: RESULTS AND DISCUSSION

Continuous Instrumentation . . . . .	64
Integrated 24-hour Filter Methods . . . . .	91
Integrated 24-hour Filter Methods to Continuous Methods . . . . .	93
CHAPTER FIVE: SUMMARY AND CONCLUSIONS . . . . .	99
REFERENCES . . . . .	104

## LIST OF TABLES

Table 1. List of Continuous Instrumentation . . . . .	38
Table 2. Thermal Optical Analysis Protocols . . . . .	55
Table 3. R-Squared Values between Continuous Methods . . . . .	72
Table 4. Slopes Values between Continuous Methods . . . . .	72
Table 5. Intercept Values between Continuous Methods . . . . .	73
Table 6. $R^2$ Values with Averaging Time of 24-hours . . . . .	94
Table 7. Slope Values with Averaging Time of 24-hours . . . . .	94
Table 8. Intercept Values with Averaging Time of 24-hours . . . . .	95

## LIST OF FIGURES

Figure 1. South Coast Air Basin PM <sub>2.5</sub> 2011 Annual Average Concentrations . . . . .	2
Figure 2. Carbonaceous Components of Particulate Matter . . . . .	4
Figure 3. Interstate 710 Air Quality Monitoring Site Location . . . . .	35
Figure 4. Relation of Relative Concentrations and Distance from Interstate 710 . . . . .	36
Figure 5. Distant and Close-up Picture of the Manifold and Sampling Ports . . . . .	39
Figure 6. Sunset Carbon Analyzer . . . . .	41
Figure 7. Simplified Block Diagram of Sunset Analyzer . . . . .	42
Figure 8. Schematic of the Aethalometer . . . . .	44
Figure 9. Legacy Aethalometers AE22 (left) and AE42 (right) . . . . .	46
Figure 10. Dual Spot Aethalometer . . . . .	47
Figure 11. Aethlabs Micro-aethalometer . . . . .	48
Figure 12. Schematic of Multiangle Absorption Photometer . . . . .	49
Figure 13. Picture of the Multiangle Absorption Photometer . . . . .	50
Figure 14. Front Display of Photoacoustic Extinctionmeter . . . . .	51
Figure 15. Schematic the Photoacoustic Extinctionmeter . . . . .	52
Figure 16. Speciation Air Sampling Systems for Integrated Filter Collection . . . . .	53

Figure 17. Desert Research Institute Model 2001 Carbon Analyzer . . . . .	56
Figure 18. Schematic of Desert Research Institute Carbon Analyzer . . . . .	58
Figure 19. Magee Scientific Optical Transmissometer . . . . .	60
Figure 20. Effects of Averaging Time on Instrument Comparisons . . . . .	67
Figure 21. Comparison of Continuous Methods . . . . .	70
Figure 22. Correlation of Legacy Aethalometers . . . . .	74
Figure 23. Correlation of Legacy and Dual Spot Aethalometer . . . . .	75
Figure 24. Spot Loading Effect: Aethalometers . . . . .	76
Figure 25. Correlation of Multiple Angle Absorption Photometer and Dual Spot Aethalometer . . . . .	78
Figure 26. Correlation of Sunset Carbon Analyzer to Multiple Angle Absorption Photometer . . . . .	82
Figure 27. Correlation of Photoacoustic Extinctionmeter and Dual Spot Aethalometer . . . . .	85
Figure 28. Correlation of Legacy and Micro Aethalometers . . . . .	88
Figure 29. 1-minute Data Noise: Legacy and Dual Spot Aethalometer . . . . .	89
Figure 30. Integrated Elemental Carbon and Integrated Black Carbon . . . . .	92
Figure 31. Sunset Carbon Analyzer and Integrated Elemental Carbon . . . . .	96

Figure 32. Legacy Aethalometers and Integrated Black	
Carbon . . . . .	98

## CHAPTER ONE

### INTRODUCTION

#### Background

Air pollution can adversely affect public health and critical functions of the atmosphere, and it is a problem throughout the United States especially in urban locations. Under the Clean Air Act (CAA) last amended in 1990, the United States Environmental Protection Agency (USEPA) has established air quality standards for six common air pollutants: carbon monoxide, lead, nitrogen dioxide, ozone, particle pollution, and sulfur dioxide. These standards are labeled as the National Ambient Air Quality Standards (NAAQS; <http://www.epa.gov/air/criteria.html>). Primary and secondary standards for these six criteria pollutants are set for states and local air quality districts to attain in their respective air basins. The primary standards are set to provide public health protection which includes the health of sensitive populations like children, elderly, and asthmatics. The secondary standards are set to provide public welfare protections. This includes protecting against decreased visibility and protecting animals, vegetation, and buildings from damage. Particulate matter

(PM) is generally categorized based on its size in fine and coarse PM ( $PM_{2.5}$  and  $PM_{10}$ , respectively). Fine PM is comprised of particles with an aerodynamic diameter less than  $2.5\text{ }\mu\text{m}$ . Coarse PM is comprised of particles with an aerodynamic diameter less than  $10\text{ }\mu\text{m}$ .  $PM_{2.5}$  is usually associated the most with adverse health effects due to PM exposure. Based on a three year average of the annual arithmetic mean, the 2006 NAAQS for  $PM_{2.5}$  was  $15\text{ }\mu\text{g}/\text{m}^3$ . Figure 1 shows the South Coast Air Quality Management District (SCAQMD) monitoring network with respect to the 2006 NAAQS for  $PM_{2.5}$  ( $15\text{ }\mu\text{g}/\text{m}^3$ , annual arithmetic mean).

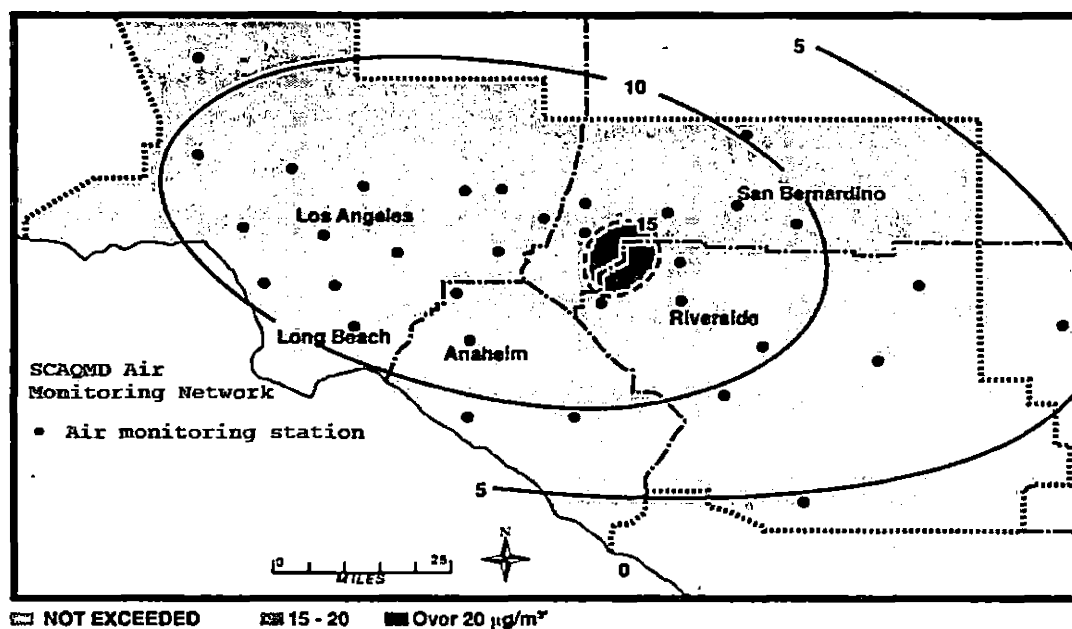


Figure 1. South Coast Air Basin  $PM_{2.5}$  2011 Annual Average Concentrations

The local air quality district is responsible for implementing plans to attain and maintain the standards by reducing PM emissions. With carbonaceous material comprising a significant portion of the PM<sub>2.5</sub> mass, local air quality regulatory agencies attempting to meet the federally established NAAQS need to reduce emissions of carbonaceous material from combustion sources. For non-attaining areas to reach attainment, understanding the chemical composition of PM is necessary to determine sources and develop adequate air pollution control devices. Understanding the effect of carbonaceous material in relation to the effect of PM<sub>2.5</sub> on the climate, public health, and environment allows air quality districts to focus on specific sources, control measures, and strategies to reduce PM and reach attainment (Rice, 2004).

### Carbonaceous Particulate Matter

Carbonaceous material represents one of the most abundant contributors to the total ambient PM mass. Chemical speciation studies attribute carbonaceous PM to account for up to 50% of the total atmospheric fine particulate mass (Tolocka et al. 2001; Seinfeld and Pandis, 1997; USEPA, 2002). Carbonaceous airborne particles are



comprised of two main components: organic carbon (OC) and elemental carbon (EC). At times, EC is also referred to as Black Carbon (BC). Of the major components that make up PM, the sampling and analysis of OC and EC are the most uncertain. This is because organic aerosols are comprised of hundreds of individual organic compounds and that OC, EC, and BC are methodologically defined species (Jacobson et al., 2000; Turpin et al., 1994). Figure 2 shows the carbonaceous components of PM.

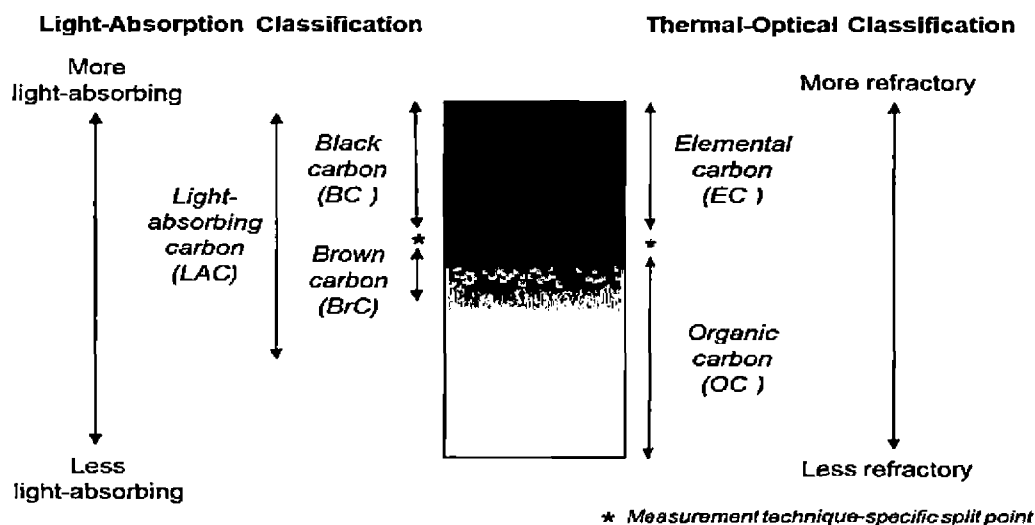


Figure 2. Carbonaceous Components of Particulate Matter  
 Source: Sasser, S.; Hemby, J.; Adler, K.; Anenberg, S.;  
 Bailey, C.; Brockman, L.; Chappell L.; DeAngelo, B.;  
 Damberg, R.; Dawson, J.; et al. Report to Congress on Black  
 Carbon; United States Environmental Protection Agency:  
 March 2012. <http://www.epa.gov/blackcarbon>. (accessed  
 January 15, 2013)

## Organic Carbon

OC is comprised of non-volatile and semi-volatile species with different thermal properties than EC. Road dust, residential wood burning, boilers, combustion processes exhaust, and gas to particle conversion of hydrocarbon gases have been found to be major sources of OC (Pandis et al., 1992). Organic material that has been collected on a sampling filter can be detected as OC through thermal/optical processes. Thermal/optical analysis methods typically define OC as the carbon evolved from a filter in a Helium only atmosphere at specific temperatures corrected for OC pyrolysis to EC. Gas chromatography/mass spectrometry has been used extensively for the determination of individual organic compounds.

## Elemental Carbon

EC is a non-volatile species with a graphitic structure, often referred to as soot. EC strongly absorbs light and is found ubiquitously in the environment. EC is mostly emitted from combustion sources. The term EC does not refer strictly to "elemental" carbon in a chemical sense, but rather is a term that is operationally defined (Andreae and Gelencsér, 2006). EC is chemically and physically stable at high temperatures and is usually

operationally defined according to the analytical method used to detect EC based on its refractory nature. The most common methods to quantify EC are thermal-optical methods in which EC is defined as the fraction of carbon, after OC oxidizes, that is oxidized in a combustion process above a certain temperature threshold in the presence of an oxygenated atmosphere (Andreae and Gelencsér, 2006).

#### Black Carbon

The terms BC and EC are often used interchangeably, although these are two different methodologically defined species. The quantities of EC and BC are not measures of the same properties of  $PM_{2.5}$  (Jeong et al., 2004). Unlike EC, BC is defined according to the light absorbing properties of carbonaceous aerosols. The most common methods to quantify BC are optical methods using transmittance, reflectance, and absorption. With the focus changing from BC as a pollutant to BC as a significant driver for global warming, the optical methods provide valuable data on the light absorbing properties of carbonaceous PM. BC is also referred to as soot. The climate effects of the soot portion of the carbonaceous PM depend on the physical and chemical properties along with its residence time and distribution in the atmosphere

(Jacobson, 2001). Black carbon is a good indicator or tracer for diesel particulate matter as it is inert in the atmosphere. It should be noted that brown Carbon (BrC) is a sub set of organic carbon compounds that absorbs light in the visible and ultraviolet range. BrC may bias measurements of BC and EC. This is especially true with aerosols that are highly polluted by biomass burning in which the ratio of BrC to BC is relatively high (Andreae and Gelencsér, 2006; Yang et al., 2009).

Light Absorbing Carbon (LAC). This term is general in nature and is used to represent light absorbing carbonaceous matter in atmospheric aerosols. Throughout this document, LAC will be used as a general term for light absorbing carbonaceous aerosols when not referring specifically to either EC or BC.

#### Primary Sources of Light Absorbing Carbon

Atmospheric LAC is emitted by both natural and anthropogenic sources through the incomplete combustion of fossil fuels and biomass. No secondary reactions for the production of BC are known to exist in the atmosphere (Hansen et al. 1984). According to a 2010 BC emission inventory for California, the top four sources for BC are on-road diesel vehicles, off-road diesel sources, on-road

gasoline vehicles, and residential coal combustion (Chow et al., 2010). The majority of BC in Southern California has been attributed to diesel PM emissions. The State of California considers diesel PM as a specific air toxicant. Studies (e.g. Fruin et al., 2008 and Zhu et al., 2002a & b) have shown that BC concentrations along freeways are an order of magnitude higher than ambient concentrations away from freeways. Fruin et al. (2008) found the causal factor for the increased concentration of BC to be statistically accounted for by truck density and total truck counts. The variability of increased BC was found to be independent of total vehicle traffic volumes while hour of day and truck volume accounted for 60-70% of the variability observed between freeway concentrations and non-freeway concentrations. The results show a strong association between heavy-duty diesel truck counts and BC concentrations. Through the use of mobile air quality platforms, Kozawa et al. (2009) found that the highest localized air pollution impacts of BC in the Los Angeles Basin were due to heavy-duty diesel trucks.

The lifecycle of BC in the environment can range from several days to several weeks dependent on meteorology (Seinfeld and Pandis, 1997). Since BC does not decompose or

degrade by atmospheric reactions or conditions, its only significant sinks are wet and dry deposition (Seinfeld and Pandis, 1997).

### Climate Effects

Light absorbing carbon affects the climate by way of three different mechanisms. First, LAC directly absorbs sunlight. LAC has the highest direct radiative forcing effect per unit mass of all possible forms of PM. BC can absorb a million times more energy than CO<sub>2</sub> per unit mass (Bond and Sun, 2005). These dark particles absorb solar radiation and then radiate energy that heats the surrounding air molecules. For regions affected by combustion emissions, BC is a significant warming pollutant. Jacobson (2001) rates light absorbing particles as the third most important and influential greenhouse contributor. Secondly, through the deposition of LAC on ice and snow, the reflectivity or the albedo of the snow and ice is changed in a manner that increases the rate of ice and snow melt. Lastly, carbonaceous particles in the atmosphere can play a role as condensation nuclei in cloud formations. The reflectivity of clouds, lifetime, and precipitation produced by clouds are affected by the presence of carbonaceous PM acting as condensation nuclei.

The result is either a warming or cooling effect, but the extent of such effect is still not fully understood. If cloud reflectivity and lifetime increase with aerosol LAC acting as condensation nuclei, an overall cooling influence on the climate will be observed (Sasser et al., 2012). LAC particles in clouds may absorb light energy and increase the temperature of the cloud causing shorter atmospheric lifetimes and reduced production of precipitation (Ackerman, 1981; Sasser et al., 2012).

#### Environmental Effects

LAC plays a role in visibility impairment and in the production of haze with aerosol PM (Watson, 2002; Seinfeld and Pandis, 1997). BC also has the potential to reduce agricultural production by decreasing the amount of sunlight that reaches crops (Chameides et al., 1999).

#### Health Effects

The SCAQMD Multiple Air Toxics Study III (MATES III) estimates that diesel PM (composed of an EC core coated by organic compounds, sulfate, nitrate, metals and other trace elements) is accountable for more than 80% of the total cancer risk from air toxics in the South Coast Air Basin (MATES III, 2008). BC has been linked through epidemiological studies to various respiratory health

outcomes such as airway inflammation (Delfino et al., 2006), asthma and bronchitis symptoms (Kim et al., 2004), and hospital admissions for respiratory effects (Ostro et al., 2009).

### Measurement Techniques

Measurement methods can be divided between continuous and non-continuous techniques. Non-continuous (or integrated) measurement methods involve collecting PM samples on a filter (usually for a period of 24-hours) and transporting the filter to a laboratory for subsequent analysis. OC and EC are typically quantified using thermal-optical methods, which can be both integrated and semi-continuous. BC is typically measured by continuous instruments with the majority of BC monitors being optical methods. Continuous and semi-continuous instruments provide data with high time resolution varying from one minute to one hour. These instruments include the aethalometer, the multiangle absorption photometer (MAAP), the photoacoustic extinctionsmeter (PAX), and the semi-continuous carbon aerosol analyzer. This is not a comprehensive list of BC and EC monitors.



## Purpose and Objectives

The purpose of this project is to compare the performance and results of different EC and BC measurement methods. The performance of the BC and EC instruments will be evaluated. The effects of environmental and operational conditions such as relative humidity and fluctuations in temperature on the instruments will be investigated.

## Scope and Significance

A comprehensive comparison between BC and EC instruments has not been performed prior to this study. Several of the instruments are recently released models that have not been previously compared to other continuous analyzers. Many researchers since the 1980's have compared instruments and methods that determine OC, EC, and BC. These previous studies have established a foundation upon which this research will expand. The results of a portion of these studies will be discussed in the literature review in Chapter 2. The significance of the project is the emerging and growing air quality concerns over diesel PM and combustion particulates. These important PM fractions are gaining notoriety with recent studies pointing towards their increased involvement in adverse health effects and

cancer risks (SQAQMD, 2008). Time resolved carbon data is required to understand the complexity of carbonaceous aerosols, determine sources, develop accurate air quality models, develop adequate control strategies, and understand the effect of carbonaceous particles on the environment and human health (Rice, 2004). Before these continuous and semi-continuous instruments can be utilized in routine monitoring networks, method demonstrations and comparisons studies must determine how they compare with one another and with standard integrated filter methods.

#### Definitions of Terms

This section is established primarily as a reference for acronyms used throughout the text. Short definitions will be provided for the some of the terms.

- Attenuation (ATN) The loss in intensity of light through a filter due to particle collection.
- Aethalometer (AE) continuous filter based optical instrument for determining black carbon
- Aethalometer model 22 (AE22) Rack mount aethalometer
- Aethalometer model 42 (AE42) Portable aethalometer
- Aethalometer model 51 (AE51) Micro aethalometer

- Aethalometer model 633 (AE633) Dual Spot Aethalometer
- Black Carbon (BC) the most strongly light-absorbing component of fine particulate matter which is formed by incomplete combustion, typically measured through optical techniques
- Brown Carbon (BrC) light absorbing organic matter that is not black carbon
- Chemical Speciation network (CSN) Thermal optical analysis for determining OC, EC, and TC
- Clean Air Act (CAA) the federal Act that regulates air emissions from area, stationary, and mobile sources and limits the emission of pollutants into the atmosphere to protect human health and the environment
- Desert Research Institute (DRI) the environmental research institute of the Nevada System of Higher Education
- Diesel Particulate Matter (DPM) the particles emitted from the exhaust of diesel fueled compression ignition engines
- Elemental Carbon (EC) the fraction of carbon oxidized above a certain temperature in the presence of oxygen and typically measured by thermal optical analysis

- Federal Reference Method (FRM) method of sampling and analyzing ambient air for air pollutants as specified as a reference method in Federal Regulations
- Fine Particulate Matter (PM<sub>2.5</sub>) particles with an aerodynamic diameter less than 2.5 µm
- Interagency Monitoring of Protected Visual Environments (IMPROVE\_A) Thermal optical analysis for measuring OC, EC, and TC using filter reflectance to correct for OC charring
- Light Absorbing Carbon (LAC) general term for light absorbing carbonaceous aerosols
- Light transmission method (LTM) determination of BC through light transmission of an integrated filter sample.
- Multiangle absorption photometer (MAAP) continuous filter based optical instrument for measuring BC
- National Ambient Air Quality Standards (NAAQS) standards established by USEPA under CAA that set limits for outdoor air pollution levels
- National Institute of Occupational Safety and Health (NIOSH) Thermal optical analysis for measuring OC, EC, and TC using filter transmittance to correct for OC charring

- Organic Carbon (OC) the carbon evolved from a filter in a Helium only atmosphere at specific temperatures and usually corrected for OC pyrolysis to EC
- Particle light absorption ( $b_{ap}$ ) light absorption due to particles in an aerosol
- Particulate matter (PM) air pollutant that refers to any material other than pure water that exists in the atmosphere in a solid or liquid state
- Photoacoustic Extinctionmeter (PAX) Photoacoustic instrument for measuring BC
- Relative Humidity (RH) ratio of the partial pressure of water vapor to the saturated vapor pressure of water at a certain temperature
- South Coast Air Quality Management District (SCAQMD) government regulatory agency for the South Coast Air Basin with authority to regulate stationary, indirect and area sources of air pollution within the basin.
- Speciation Air Sampling Systems (SASS) portable integrated ambient particulate sampling system designed to comply and exceed USEPA's speciation requirements

- Specific attenuation ( $\sigma_{\text{ATN}}$ ) value of ATN per unit mass of BC; converts the measurement of ATN on a filter into BC mass
- Thermal-optical analysis (TOA) analysis for measuring OC, EC, and TC based on refractory nature and light absorbing nature of carbon
- Thermal-optical reflectance (TOR) a TOA using filter reflectance to correct for OC charring
- Thermal-optical transmittance (TOT) a TOA using filter transmittance to correct for OC charring
- Total Carbon (TC) the sum of both the EC and OC fractions
- United States Environmental Protection Agency (USEPA) federal agency in charge of setting policy and guidelines to protect national interests in environmental resources

## CHAPTER TWO

### LITERATURE REVIEW

Several thermal, optical, and thermal-optical methods to determine EC and BC exist, but only a few comparison studies attempted to investigate the observed differences in EC and BC measurements. Watson et al. (2005) summarized some of these comparison studies and found EC and BC measurement differences of a factor of two to be common between methods. This literature review will focus on previous comparison studies of EC and BC determination methods. The literature review will be structured into three sections: comparisons between continuous methods, comparisons between integrated filter methods, and comparisons between integrated and continuous methods.

#### Comparisons among Continuous Methods

##### Aethalometer Comparisons

During a study at the Fresno Supersite in California from January through December 2000, Watson and Chow (2002) compared a single wavelength and a 7 wavelength aethalometer and found the two to be highly correlated with  $r = 1$  and a slope of 0.89. The 7 wavelength aethalometer

results were on average 9% lower than the single wavelength aethalometer. The largest differences between the two aethalometers were found at times when the BC concentrations were the highest. The frequency of filter tape advances on the 7 wavelength aethalometer was about twice as many as the single wavelength aethalometer resulting in an increase of data loss for the 7 wavelength model.

During a study at the Fresno Supersite in California from December 2003 through November 2004, Park et al. (2006) found a strong correlation between co-located two wavelength and seven wavelength aethalometers with time average of one month (regression slope range 1.03 to 1.14; intercept range 0.00 to 0.09  $\mu\text{g}/\text{m}^3$ ;  $r^2 > 0.97$ ). The differences between the two instruments did not vary significantly between the different seasons.

During a study in Riverside CA from July to August 2005, Snyder and Schauer (2007) compared two seven wavelength aethalometers with each other under different flow settings (5.0 and 5.9 L/Min). A high correlation for particle light absorption between the two aethalometers at 880nm was found with a  $R^2$  value of 0.92 and a slopes value of 1.01. Even with different flow settings and the higher



flow aethalometer having a greater frequency of filter spot changes, no significant differences were noticed between the two aethalometers. The authors suggested the effects of filter loading artifacts to be minor in urban environments. Snyder and Schauer (2007) concluded that the ratio of attenuation to EC mass was not constant, but varied in a predictable diurnal pattern for weekdays. The variation in the specific attenuation,  $\sigma_{\text{ATN}}$ , appeared to be related to changes in the bulk composition of carbonaceous aerosols and changes in the wavelength dependence of light attenuation. The variation in the  $\sigma_{\text{ATN}}$  for the aethalometers was found to range from 25.58 to 35.31 m<sup>2</sup>/g at the Riverside, CA site location. Snyder and Schauer (2007) found that the largest single factor to produce differences of attenuation between filter based optical methods is the type of filter utilized. Particles that collect on a filter material penetrate the fibers of that filter material and are then exposed to an intensity of illumination that is increased by multiple reflections at the microscopic scale within the matrix of fibers. The properties of quartz fiber differ significantly from Teflon glass fiber filter materials.

### Dual Spot Technology Aethalometer

The AE633 dual spot aethalometer is a newly released instrument for measuring BC, and prior to this study it has not been featured in previous instrument comparisons. The dual spot technology aethalometer is designed to improve BC measurement performance by eliminating aerosol loading effects that affect the older aethalometers.

### Aethalometer to Multiangle Absorption Photometer

The MAAP compensates for back-scattering and multiple-scattering through a radiative transfer model by measuring both reflectance and transmittance (Petzold, et al., 2005). In comparing a 7 wavelength aethalometer to MAAP BC data at the Fresno Supersite, Park et al. (2006) found the instruments to agree within 3% during the summer season and within 10-20% during the winter season.

From August 1 to September 30, 2005 at the Fresno supersite, Chow et al. (2009) found 24 hour average BC data from a seven wavelength aethalometer (660nm) and MAAP (670nm) to agree to within 1%. The aethalometer data was corrected with methods outlined in Arnott et al. (2005). The regression slope between the MAAP (Y) and the aethalometer (X) for 24-hour average BC was  $1.00 \pm 0.02$  and intercept of  $0.00 \pm 0.03$  and an  $R^2 = 0.99$ . The correlation

between the methods decreases with an averaging time of one hour. The aethalometer (y) and the MAAP (x) were found to have a slope value of 1.19, intercept value of -1.41, and  $R^2$  of 0.97.

#### Sunset Carbon Analyzer

During a study at the Gosan site in Korea from March 24 to April 5, 2007, Bae et al. (2007) compared two Sunset semi-continuous carbon analyzers running different thermal protocols for determining carbon content through thermal optical analysis (TOA). The differences in max temperature, number of steps, and hold times of the two thermal methods were found to affect the correlations of OC between methods. Between the two thermal protocols, EC showed good agreement with a slope of  $1.05 \pm 0.15$  and an  $R^2 = 0.98$ . The results of this study indicate that EC is not seriously affected by small differences in the thermal protocol with maximum temperature, number of thermal steps, and hold times in carbon TOA.

#### Sunset Carbon Analyzer to BC Instruments

Jeong et al. (2004) compared EC from a Sunset semi-continuous instrument to an aethalometer at two sites. The comparison study at Philadelphia, Pennsylvania was from July 1 to August 2, 2002 while the study at Rochester, New

York was from June 6 - 18 2002. The results from the aethalometer BC using a fixed  $\sigma_{\text{ATN}} = 16.6 \text{ m}^2\text{g}^{-1}$  were found to be significantly higher than Sunset thermal EC at both sites. The correlation between thermal EC and BC varied significantly between the two sites. The Philadelphia, PA site was subject to high concentrations of wood smoke from a Canadian forest fire during the sampling period which would be large causal factor for the difference in correlations between the sites. An  $R^2$  value of 0.84 and slope value of 3.3 was found in Rochester, NY while an  $R^2$  value of 0.60 and slope value of 2.7 was found at Philadelphia, PA. These slopes are significantly higher than the slope obtained when comparing Sunset BC (y) to Sunset thermal EC. The decrease in the proportional nature between Sunset EC and Aethalometer BC shows the variability in the absorption coefficient used to convert ATN to BC mass for the aethalometer.

Snyder and Schauer (2007) compared two 7 wavelength Aethalometers (AE31) to a Sunset semi-continuous carbon analyzer. The correlation of the particle light absorption of the aethalometer (880nm) to Sunset EC was found to be strong with an  $R^2$  value of 0.87.

As mentioned earlier, the Sunset carbon analyzer also measures optical BC concentrations by measuring light transmission at 670nm during the particle collection phase. Jeong et al. (2004) found the correlation between the Sunset thermal EC and the Sunset optical BC to vary by location. In comparing thermal EC to optical BC, the correlation at Rochester, NY was  $R^2 = 0.95$  with a slope of  $0.89 \pm 0.02$  and at Philadelphia, PA was  $R^2 = 0.73$  with a slope of  $0.99 \pm 0.07$ . At both locations, thermal EC was found to be higher than the Sunset optical BC measurement.

Chow et al. (2009) found that the Sunset optical BC measurements correlate well with the MAAP ( $R^2 = 0.99$ ) and the Aethalometer ( $R^2 = 0.94$ ) for 24 hour average BC concentrations. With the Sunset optical BC as y axis, the slope value between the methods was 0.59 for both the MAAP and aethalometer. The Sunset optical measurements were found to be 47% less than a 7 wavelength aethalometer BC (660nm) and 49% less than MAAP BC (670nm).

#### Photoacoustic Extinctionmeter Literature

The PAX is a newly commercialized instrument that has not been previously included in BC or EC instrumentation comparison studies. There are other photoacoustic BC

continuous instruments that have been used in prior instruments comparisons that will be briefly addressed.

Using a Desert Research Institute (DRI) photoacoustic instrument (PA) as a benchmark for in-situ particle light absorption ( $b_{ap}$ ), Chow et al. (2009) compared several filter based BC instruments measuring particle light absorptions. The MAAP overestimated  $b_{ap}$  by 51% in comparison to PA  $b_{ap}$ . Unadjusted aethalometer data overestimated  $b_{ap}$  by 4.7 to 7.2 times the PA  $b_{ap}$ . The differences are accounted to filter matrix, filter loading, back scattering, and multiple scattering. The adjusted aethalometer  $b_{ap}$  using published algorithms (Arnott et al., 2005) was found to be 24 to 69% higher than PA  $b_{ap}$ . In comparing aethalometer BC data to DRI PA aerosol light absorption at Big Bend National Park in South Texas from July through October 1999, Arnott et al. (2003) found the correlation to be reasonably well with times of agreement and disagreement between the two methods. Differences were proposed to be due to limits of detection between the methods and compositional changes in the aerosol. Arnott et al. (2003) found that when RH is greater than 70%, a systematic decrease in the measurement of light absorption by PA occurred.

### Limitations of Continuous Filter Based Methods

Continuous instruments that involve collecting particles on a filter and measuring the particle light absorption ( $b_{ap}$ ) are subject to three potential artifacts that may affect the  $b_{ap}$  reading. These instruments include the various aethalometers and the MAAP. First back scattered light from particles in the filter, second the enhancement of multiple scattering by highly diffusive filter material and by particles on or embedded in the filter, and lastly the reduction of multiple scattering by increased particle loading and particle light absorption are the three potential artifacts affecting filter based continuous BC analyzers (Chow et al., 2009).

The specific attenuation,  $\sigma_{ATN}$ , utilized to convert ATN to BC mass has been suggested (Petzold et al., 1997; Lioussse et al., 1993; Snyder and Schauer, 2007) to be variable according to location, time of day, season of year, particle size, mass fraction, and carbon source. These studies suggest a site specific and time specific  $\sigma_{ATN}$  should be determined to convert ATN to BC mass. The MAAP compensates for back-scattering and multiple-scattering through a radiative transfer model by measuring both reflectance and transmittance (Petzold, et al., 2005). The

legacy aethalometers do not account for back and multiple scattering effects and therefore adjustments may be made to Legacy Aethalometer data by procedures outlined in Arnott et al. (2005). The dual spot technology AE633 aethalometer compensates for particle loading effects.

### Comparisons among Integrated Methods

#### Comparison between Thermal Optical Methods

Using the same IMPROVE\_A thermal protocol, Chow et al. (2009) compared EC concentrations of IMPROVE\_A TOT with IMPROVE\_A TOR. On average, the results from a TOT method were found to be 23% less than results from a TOR method for 24 hour EC concentrations. The ordinary least squares regression slope with TOT (y) and TOR (x) was  $0.71 \pm 0.04$  with an intercept of  $0.05 \pm 0.04 \mu\text{g}/\text{m}^3$ . The correlation between TOT and TOR is strong with an  $R^2$  value of 0.95 indicating linearity across high and low concentrations.

#### Integrated EC to Integrated BC

Ahmed et al., (2009) compared Magee Scientific Transmissometer BC results on quartz Whatman 41 filters to thermal optical TOT method using the NIOSH protocol. The monthly averages of optical BC and thermal-optical EC values at 4 sites resulted in a regression line passing



through the origin with a slope of 0.91 and a regression coefficient of  $R^2 = 0.84$ . The transmissometer BC results were found to be lower than the integrated EC TOT using the NIOSH protocol.

At seven sites, Neil et al. (2009) analyzed Federal Reference Method (FRM) Teflon filters with a Magee Scientific Transmissometer and compared to EC determined by TOT. The results for seven Air Quality sites showed high correlation at  $R^2 = 0.89$ . The relationship between optical attenuation and thermal EC measurements was found to vary by site location. The slope between optical attenuation and thermal EC, which represents the specific attenuation coefficient, varied between sites with the variance attributed to source of PM (wood smoke sources and non-wood smoke sources). At four sites, Neil et al., 2009 compared the transmissometer ATN to integrated TOR IMPROVE EC method and found the correlation to be strong with  $R^2 = 0.93$ . Using a Magee Scientific Transmissometer with FRM Teflon filters, the  $\sigma_{ATN}$  for converting ATN to BC mass was found to be between 10 and 11  $m^2/g$  (Neil et al., 2009).

## Comparisons between Integrated and Continuous Methods

### Integrated EC to Sunset Thermal EC

Bae et al. (2004) found the results of a semi-continuous Sunset carbon analyzer to be comparable to integrated filter TOA EC. Linear regression comparing 24 hour average Sunset EC data to daily integrated samples shows the slope to be  $0.95 \pm 0.05$ . A low coefficient of regression for EC at 0.60 was attributed to dispersion of the data due to the large number of measurements near the EC detection limit.

Snyder and Schauer (2007) found that the methods to determine EC by a Sunset Laboratory semi-continuous carbon analyzer (y) to Integrated Filter EC (x) to correlate well with a  $R^2 = 0.90$ . The slope of the linear regression is  $1.11 \pm 0.05$ . On average, the two methods varied by less than 15%.

For 24 hour average BC concentrations, the Sunset EC was found to be 45% less than 24 integrated filters analyzed by IMPROVE\_A TOR (Chow et al., 2009). The ordinary least squares regression equation with Sunset EC as y and IMPROVE\_A TOR as x has a slope of  $0.62 \pm 0.05$ , an intercept of  $-0.05 \pm 0.06 \mu\text{g}/\text{m}^3$ , and an  $R^2$  value of 0.87.

### Integrated EC to Aethalometer BC

Park et al., (2010) compared aethalometer BC results from an aethalometer at 880 nm to 24 hour integrated samples analyzed for EC using TOT. Discontinuities in the aethalometer data was seen at filter spot changes with a rise in BC concentration after the filter tape advanced. The aethalometer data was corrected by an empirical method to correct for the optical saturation effect. The linear regression of compensated aethalometer BC (x) to 24 hour integrated EC (y) concentrations shows excellent agreement with a slope of  $1.06 \pm 0.04$ , intercept of  $0.05 \pm 0.24$ , and  $R^2$  of 0.98. The non-compensated data linear regression BC data to 24 hour integrated EC shows a lower slope of  $0.88 \pm 0.04$ , intercept of  $0.04 \pm 0.20$ , and an  $R^2$  of 0.98. This study concluded that the relationship between attenuation and BC was non-linear at their sample locations. Park et al. (2006) examined a 7 wavelength aethalometer for two time periods; December 2003 to February 2004 and June 2004 to August 2004. The aethalometer BC was found to be less than the IMPROVE EC, and their regression slope was 1.49 for the December to February time period and 1.09 for the June to August time period.

At the Fresno Supersite, Watson and Chow (2002) found that a 2 wavelength and a 7 wavelength aethalometer were on average 25 and 31% lower than integrated filter EC concentrations. The measurements between the aethalometers BC and filter EC were found to be predictable with correlation coefficients exceeding 0.90.

A study (Allen et al., 2009) in Uniontown, PA during the summer of 1990 compared aethalometer BC concentration to 3-hr integrated filter samples analyzed by TOR. The results of BC and EC concentration were found to be highly correlated with an  $R^2 = 0.92$  and a regression equation of  $BC (\mu g m^{-3}) = 0.95(\pm 0.04) EC - 0.2(\pm 0.4)$ .

In a study at Research Triangle Park in Durham, NC from July to 2 October 2002, Rice (2004) found the correlation of aethalometer BC to integrated EC TOT method to be 0.89 with a regression equation of  $BC = 1.17 \pm 0.16$  TOT EC +  $0.06 \pm 0.10 \mu g C m^{-3}$ .

#### Integrated EC to Multiangle Absorption Photometer

Park et al. (2006) compared MAAP BC and IMPROVE EC for two time periods; December 2003 to February 2004 and June 2004 to August 2004. The MAAP was found to be less than IMPROVE EC with a regression slope of 1.16 for the December

to February time period and more than IMPROVE EC with a slope of 0.94 for the June to August time period.

### Summary

Several methods are used to measure the atmospheric concentrations of EC and BC. Differences between these methods lead to discrepancies between the observed EC and BC results. In the majority of instrument comparison studies, the BC/EC correlations are typically strong. In looking at a number of inter-comparisons studies, the USEPA summarized that BC and EC measurements have consistently high correlations with average  $R^2$  value between the methods they summarized to be  $0.86 \pm 0.11$  (Sasser et al., 2012). However, the BC/EC correlation slope usually deviates from a 1:1 relationship. Specifically, the BC/EC ratios for 70% of the summarized comparisons were within 30% of a 1:1 relationship with BC/EC ratios ranging from 0.7 to 1.3. However, in some cases ratios with as low as 0.5 and as high as 2 were also observed (Sasser et al., 2012).

Among comparison studies, a lack of consistency exists with the processing of the raw data measurements, which can also produce variability between studies (Sasser et al., 2012).

In addressing the prior research as a whole, it can be concluded that the differences between methods are not consistent among the comparison studies. BC and EC measurements are affected by changes in PM composition, atmospheric temperature and humidity, and other atmospheric variations. Furthermore, the aerosol analyzed in field studies cannot be systematically varied with respect to composition, size distribution, mixing state, source, relative humidity, and other variables to understand how these factors affect the measurement of aerosol properties (Sheridan et al., 2005). The location of the air quality site along with type and proximity of sources for carbonaceous aerosols also has an effect on instrument response and may affect the comparison results.

## CHAPTER THREE

### METHODOLOGY

#### Site Description and Timing

This comparison study consisted of one air quality monitoring station located along the Interstate 710 freeway (I-710) in Long Beach, CA. The air quality monitoring station was sited downwind of and approximately 15 m east of the I-710 center median. Figure 3 indicates the location of the monitoring site. The eight lane interstate has four north bound and four south bound lanes. I-710 connects the ports of Long Beach and San Pedro to rail yards, local industry, warehouses, and other freeways east of Los Angeles. Heavy duty diesel trucks account for a significant percentage of the total number of vehicles on I-710. Zhu, et al. (2002a) found approximately 20-25% of the vehicle count is accountable to heavy duty diesel trucks along the I-710 corridor.

Near roadway locations have been identified as locations of increased  $PM_{2.5}$  (although the bulk of atmospheric  $PM_{2.5}$  is emitted from regional sources), ultrafine particles (UFP), BC, carbon monoxide (CO), nitrogen monoxide (NO), and other primary combustion

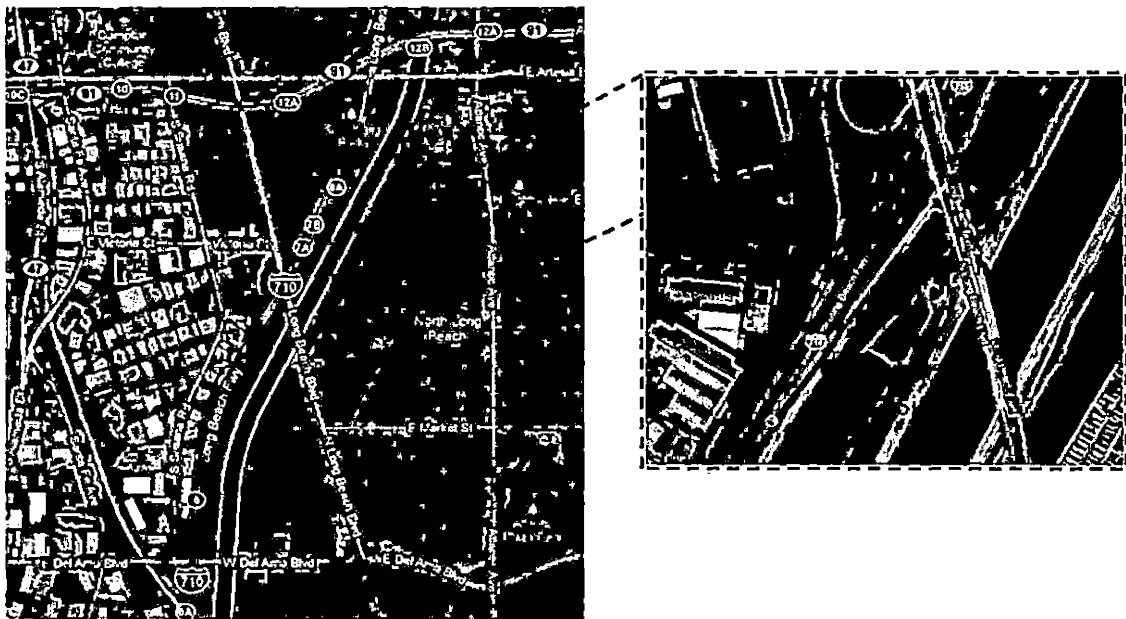


Figure 3. Interstate 710 Air Quality Monitoring Site Location

pollutants. During a series of studies conducted near the I-405 and I-710 freeways in Southern California, Zhu et al. (2002a and b) found that particle mass, UFP, BC, and CO peaked within 20-30 m. The pollutant levels decreased to background levels after about 300 m (Fig 4). For this instrument comparison study, the proximity of the monitoring station to I-710 was ideal so that a large range of concentrations for BC and EC could be measured.

The timing of the study consisted of a five week intensive sampling period spanning from March 7 to April 8 of 2012. According to historical weather data for the City



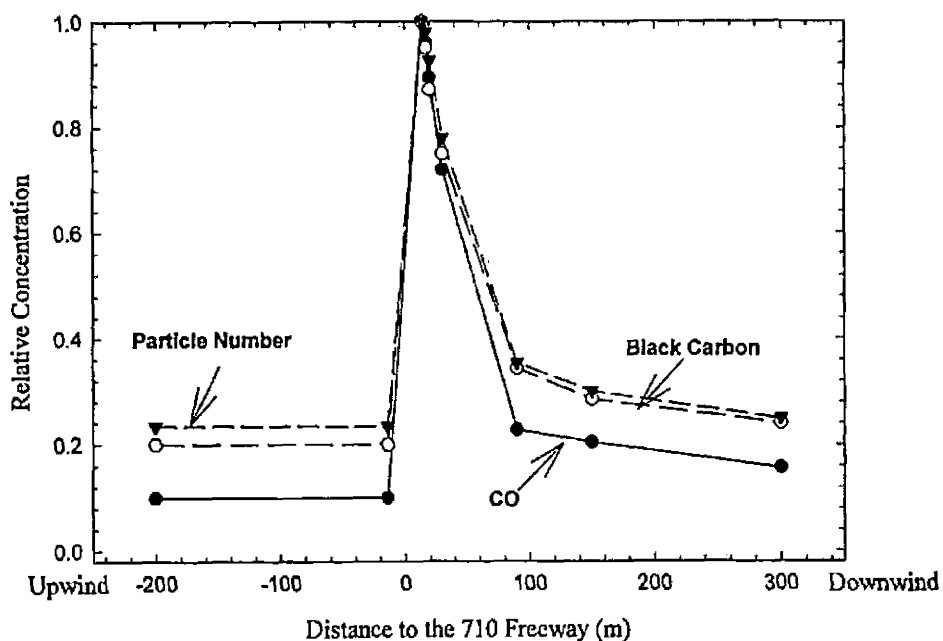


Figure 4. Relation of Relative Concentrations and Distance from Interstate 710  
Source: Zhu, Y.; Hinds, W.; Kim, S.; Shen, S.; Sioutas, C. Study of Ultrafine Particles near a Major Highway with Heavy-duty Diesel Traffic. *Atmos. Environ.* 2002a, 36, 4323-4335.

#### Instrumentation

Seven continuous analyzers, one semi-continuous thermal/optical carbon analyzer, and three Speciation Air Sampling Systems (SASS) were set-up and run concurrently at the I-710 site. The SASS units were utilized to collect daily 24 hour integrated Teflon and quartz filter samples for further laboratory analysis. Data for meteorological conditions such as wind speed, wind direction, relative

humidity, and outside temperature was collected for the duration of the study. Carbon dioxide (CO<sub>2</sub>) concentrations were continuously monitored throughout the study. Data for vehicle count and truck counts was obtained from the California Department of Transportation (<http://pems.dot.ca.gov>).

### Continuous Instrumentation

The line-up of continuous and semi-continuous instruments can be seen in Table 1. These instruments were all placed online from a single sampling manifold (Figure 5). From the sampling manifold, most of the lines heading to the instruments were equipped with sharp cut cyclone to exclude PM with an aerodynamic diameter greater than 2.5 µm. Non-conductive tubing was used to connect the manifold to the various instruments. In order to minimize particle diffusion losses, the length of the tubing connecting each of the instruments to the manifold kept as short as possible and it was approximately the same length.

The continuous instruments were placed online and ran continuously for the 5 week time period with relatively little operator intervention or down time. The site was visited every two or three days to ensure all the continuous instruments were operating correctly and within

Table 1. List of Continuous Instrumentation						
Method	Units	Measurement Principle	$\lambda$ (nm)	Filter Matrix	Flow Rate (L/min)	Time Average
AE51	$b_{abs}$ ( $Mm^{-1}$ ) BC ( $\mu g/m^3$ )	Rate of change in absorption of transmitted light on filter 3 mm spot	880	T60 Teflon/ glass fiber	0.1	1 min
AE22	$b_{abs}$ ( $Mm^{-1}$ ) BC ( $\mu g/m^3$ )	Light transmission is continuously monitored. Attenuation is converted to BC	880	Quartz fiber	5	1 min
AE42	$b_{abs}$ ( $Mm^{-1}$ ) BC ( $\mu g/m^3$ )				5	1 min
AE633	$b_{abs}$ ( $Mm^{-1}$ ) BC ( $\mu g/m^3$ )	Light transmission is continuously monitored at up to $10\lambda$ . ATN is converted to BC. Employs dual spots with different flow and spot loadings. Allows instrument to address spot loading effects	880	T60 Teflon/ glass fiber	5	1 min
MAAP 5012	$b_{abs}$ ( $Mm^{-1}$ ) BC ( $\mu g/m^3$ )	Light transmission ( $0^\circ$ ) and reflectance ( $130^\circ$ and $165^\circ$ ) is monitored. Particle light absorption is calculated through a two stream approximation radiative transfer model	670	Quartz fiber	16.7	1 min
PAX	$b_{abs}$ ( $Mm^{-1}$ ) Bscat BC	Direct in-situ measurement of light absorption and scattering. Absorption measurement correlates to black carbon mass concentration	870	None	1.0	1-min
Sunset Carbon Field Analyzer	OC, EC, and TC ( $\mu g/m^3$ )  BC ( $\mu g/m^3$ )	Particles collected on filter for 47 minutes are subject to thermal/optical analysis following NIOSH 5040 TOT protocol  Light transmission through filter is monitored to quantify BC	660	Quartz fiber	8.0	60 min

the correct parameters. Flow checks were performed on all instruments at the beginning and end of the study. Details on the procedure and flow calibration factors used can be seen under the quality assurance section towards the end of the methods chapter.

The time and date on the instruments was carefully monitored throughout the study in order to adjust the data temporally to align with one another upon data analysis. Pacific Standard Time was used throughout the study and the reference time standard was set as the Sunset carbon analyzer's computer.

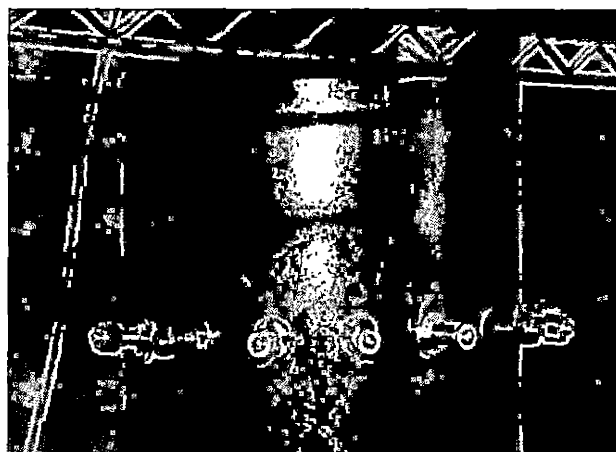
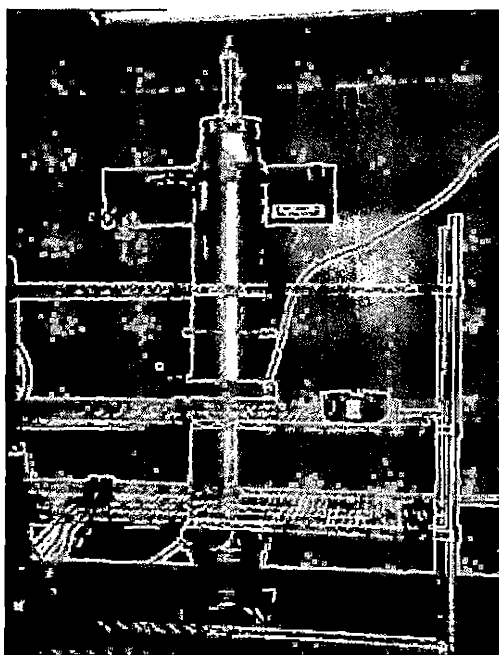


Figure 5. Distant and Close-up Picture of the Manifold and Sampling Ports

Sunset Semi-Continuous Carbon Analyzer. The Sunset Laboratories semi-continuous model 4 OC/EC analyzer measures OC and EC through a thermal-optical method and can be seen in Figure 6. The semi-continuous carbon aerosol field instrument from Sunset Laboratories (Tigard, OR, USA) has a time resolution of one hour. This instrument was developed to be a field deployable alternative to integrated filter collection and laboratory analysis for OC/EC.

A particle collection phase involves collecting particles on a quartz fiber filter for 47 minutes at a specified flow rate. The following 13 minutes of the hour are for the actual OC/EC analysis which includes an internal calibration check. The same sampling filter can be used for multiple sampling and analysis. However, due to the accumulation of Iron Oxide and other refractory materials, the sampling filter is usually replaced twice a month.

The particles collected on the filter are analyzed following the NIOSH 5040 thermal-optical transmission (TOT) protocol (Birch and Cary, 1996; NIOSH, 1996). OC evolves from the filter in a He atmosphere while a He/O<sub>2</sub> atmosphere is needed for EC to evolve. The evolved carbon is converted

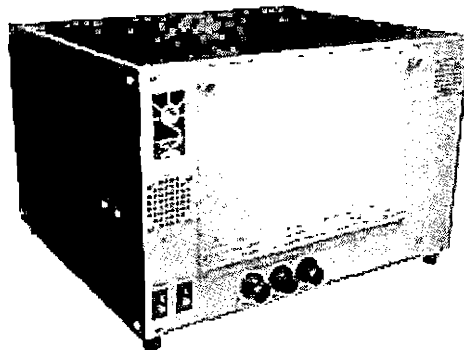


Figure 6. Sunset Carbon Analyzer

Source: Sunset Laboratory. <http://www.sunlab.com/products-services/model-4-field-analyzer.html> (accessed Jan 7, 2013).

to methane ( $\text{CH}_4$ ) and analyzed by a non-dispersive infrared (NDIR) detector. The pyrolysis of OC is corrected by laser transmittance which observes the darkening of the filter by measuring light transmittance. The split point for OC to EC is the when the laser transmittance equals the initial signal. A simplified block diagram of the Sunset semi-continuous can be seen in Figure 7.

The carbon analyzer was equipped with a carbon-strips denuder and a sharp cut cyclone. The denuder has parallel charcoal impregnated filter strips that collect semi-volatile gas phase organic compounds. This prevents organic compounds from absorbing on the downstream quartz fiber

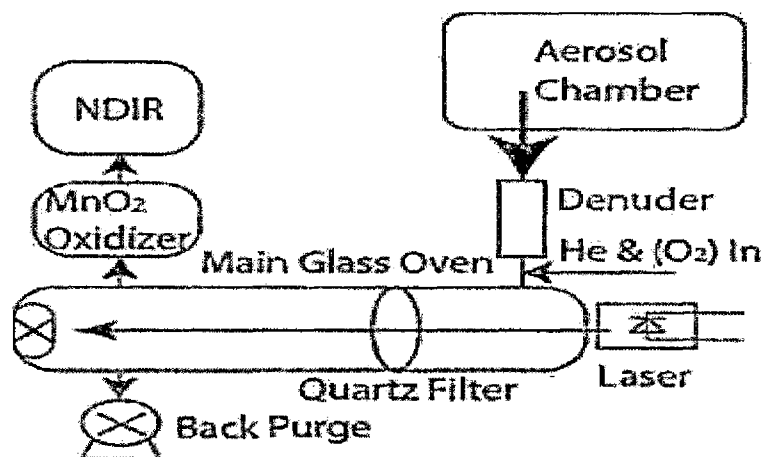


Figure 7. Simplified Block Diagram of Sunset Analyzer  
 Source: Bae, M.; Lee, J.; Kim, Y.; Oak, M.; Shin, J.; Lee, K.; Lee, H.; Lee, S.; and Kim, Y. Analytical Methods of Levoglucosan, a Tracer for Cellulose in Biomass Burning, by Four Different Techniques. *Asian J. of Atmos. Environ.* 2012, 6-1, 53-66.

filter and avoids OC sorption artifacts (Mader et al., 2003; Bae et al., 2007).

The semi-continuous OC/EC analyzer is both externally and internally calibrated. Prior to placing online, the instrument was externally calibrated using a sucrose standard stock solution. During the sampling campaign, part of the analysis phase includes an internal calibration check that is performed with a 5% methane in helium mixture injection. The internal calibration is used to compensate for the variability of the NDIR detector response with

converting the detector signal of methane into OC and EC concentrations at the end of every analysis.

The Sunset OC/EC analyzer also renders 1-min BC concentration data by measuring light transmittance (Bae et al., 2004). The change in light transmission is measured during the sample collection phase to obtain an attenuation reading. The  $\sigma_{\text{ATN}}$  to convert ATN to BC mass is dependent on the absorbance and measured thermal EC and estimated automatically by the Sunset carbon analyzer through a second degree polynomial fit. The specific attenuation decreases as the sample deposit becomes darker.

Aethalometer. The aethalometer from Magee Scientific (Berkley, CA, USA) is an automated instrument for determining BC concentrations in a non-destructive manner. Similar to OC and EC, BC is operationally defined according to the method used to initiate a signal and to transform that signal into a concentration. BC has a strong optical absorbance in the 870 to 880 nm range which is readily measured through absorbance, transmittance, or light scattering techniques.

The measurement principles of rendering BC concentrations by aethalometers involve continuously measuring the attenuation of a beam of light passing



through a filter laden with particles. With a constant air flow through the filter, the rate of deposition of BC on the filter is proportional to aerosol BC. The rate of change of optical attenuation is the basis of this BC methodology to measure the deposition of BC on a filter tape (Hansen et al, 1984). The filter tape advances at a predetermined darkness or after a set amount of sampling time. Figure 8 shows a schematic of the aethalometer.

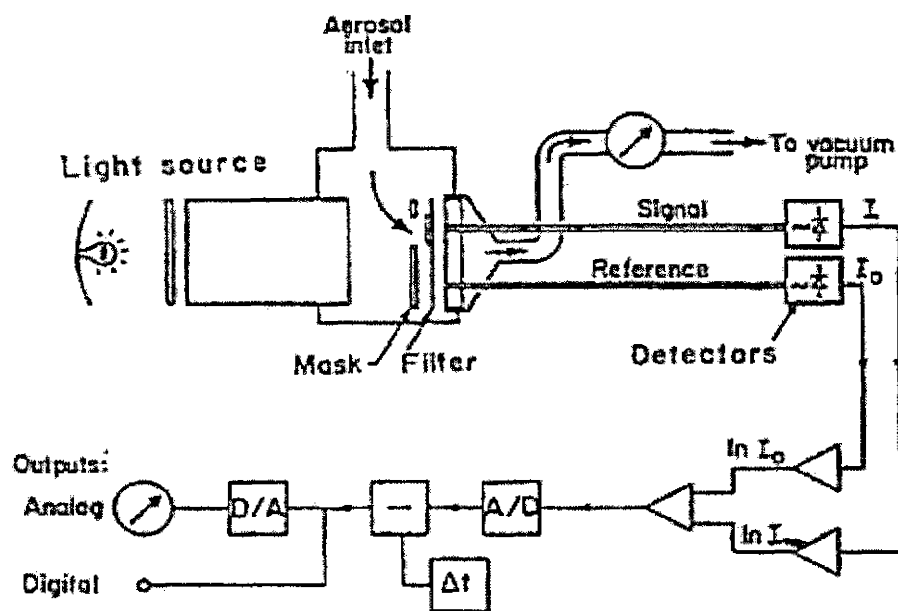


Figure 8. Schematic of the Aethalometer  
Source: Hansen, A.; Rosen, H.; Novakov, T. The Aethalometer-an Instrument for the Real-time Measurement of Optical Absorption by Aerosol Particles. *Sci. Total Environ.* 1984, 36, 191-196.

The assumptions of the aethalometer method are twofold. The first assumption is that the attenuation of light is linearly proportional to BC particles loading on a filter. The second assumption is that the relationship between attenuation and BC particle loading is constant over time (Snyder & Schauer, 2007). BC concentrations are then calculated from the rate of change of attenuation (Hansen et al., 1984). One rack (AE22), one portable (AE42), two micro (AE51), and one dual spot technology aethalometer (AE633) were utilized in this BC instrument comparison study.

The Rack Aethalometer (AE22) is a standard purchase aethalometer for use in an air quality monitoring station. The aethalometer uses a continuous optical analysis method at two wavelengths to measure light absorption on a filter media. The method is continuous, instantaneous, and non-destructive. The rack aethalometer measures quantitatively for BC at 880 nm and for aromatic organic compounds at 370 nm. The instrument converts the measured optical absorption to BC mass by dividing the ATN by the specific attenuation ( $\sigma_{\text{ATN}}$ ).  $\sigma_{\text{ATN}}$  is assumed to constant at 16.6 m<sup>2</sup>/g. The Portable Aethalometer (AE42) has the same analytical performance and instrument methodology as the Rack Aethalometer. Both

instruments had a sharp cut cyclone inline to cut out particles greater than 2.5  $\mu\text{m}$ . These two instruments (Figure 9) are referred to as the "legacy" aethalometers as result of having the same instrument methodology.

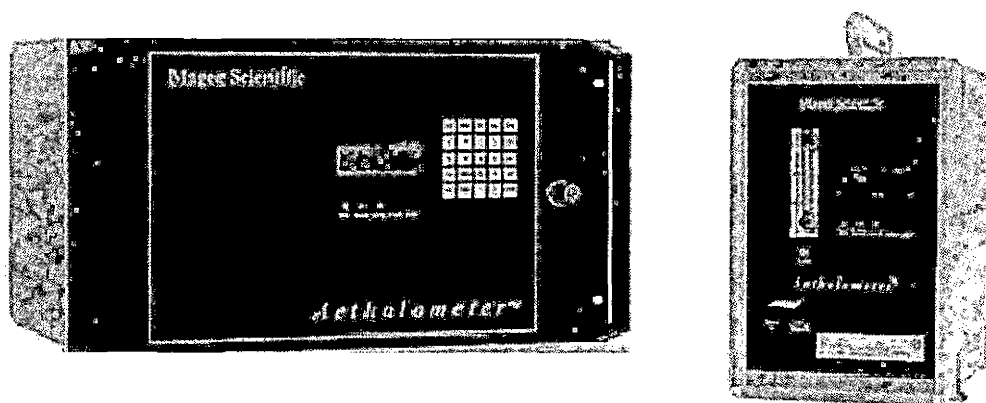


Figure 9. Legacy Aethalometers AE22(left) and AE42(right)  
Source: Magee Scientific: Air Sampling Products.  
[http://www.mageesci.com/air\\_sampling\\_products.html](http://www.mageesci.com/air_sampling_products.html)  
(accessed Jan 7, 2013)

The Dual Spot Technology Aethalometer Model AE633 (Figure 10) has been designed to adjust for known problems that affect filter based BC monitors. The filter media for the AE633 is a T60 Teflon/glass fiber filter media. The instrument is hermetically sealed which makes the unit less sensitive to fluctuations in relative humidity (RH). Fluctuations in RH occur in air quality stations as the station's air conditioning unit cycles on and off to keep

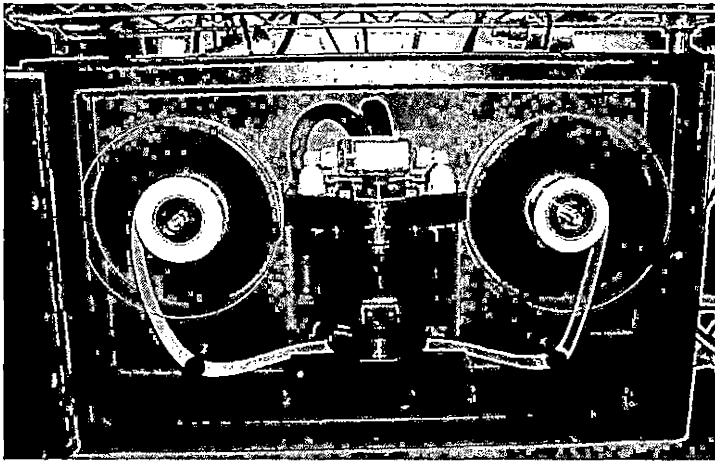


Figure 10. Dual Spot Aethalometer

the station within a specified temperature range. The instrument provides real-time absorption analysis for up to 10 optical wavelengths between UV and IR (370-950nm). When comparing to other methods for BC, 880nm wavelength was used. The patented dual spot technology involves active loading compensation by having two parallel sampling channels operating simultaneously. These parallel sampling channels are operated under different flows which produces significantly different loading rates. The data from the two channels is combined to extrapolate the ideal measurement of BC without loading effects and adjust for the loading compensation parameter ( $k$ ) in real time. The sample line from the inlet to the instrument was equipped

with a sharp cut cyclone to cut out particles larger than  $2.5\ \mu\text{m}$  (Drinovec et al., 2012).

Micro-aethalometers are considered by its manufacturer (AethLabs, San Francisco, CA) to be the world's first real-time pocket size BC aerosol monitoring device. The device which is shown in Figure 11 is designed to be worn by a person in order to measure the BC exposure of the individual. The micro-aethalometers were connected to power sources in order to run for longer than the battery life would typically allow (24-48 hours). The flow was set to 100 mL/min. These devices were not externally equipped with sharp cut cyclones. Every two to three days, the micro-aethalometers would be taken offline for the data to be downloaded and to install a new T60 filter strip.

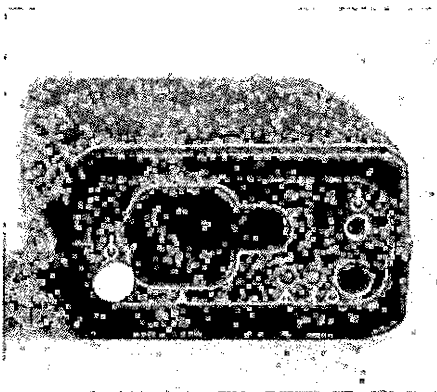


Figure 11. Aethlabs Micro-aethalometer

Multiangle Absorption Photometer (MAAP). The MAAP model 5012 from Thermo Scientific (Waltham, MA, USA) is an automated instrument that measures BC on a particle-loaded glass fiber filter. The MAAP is similar to the aethalometers in that it continuously measures atmospheric BC on a revolving filter media. The MAAP measures at 670 nm and uses multiple detectors to simultaneously measure optical absorption and scattering of light by the particles. Light transmission is continuously monitored at 0° while light reflectance is monitored from the projected light beam at 130° and 165°. A schematic of the MAAP is displayed in Figure 12.

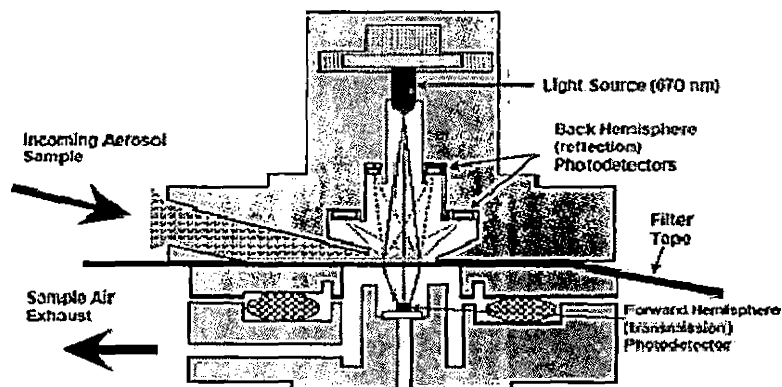


Figure 12. Schematic of Multiangle Absorption Photometer  
Source: Petzold, A.; Schloesser, H.; Sheridan, P.; Arnott, P.; Ogren, J.; Virkkula, A. Evaluation of Multiangle Absorption Photometry for Measuring Aerosol Light Absorption. *Aerosol Sci. Technol.* 2005, 39(1), 40-51.

The MAAP methodology is aimed at solving the problem that light scattering has on filter based real-time BC monitors. Both the filter matrix and the aerosol particles can scatter light which would cause an optical measurement of BC to overestimate the absorption coefficient. A two-stream approximation radiative transfer model calculates  $b_{ap}$  which is then converted to a BC concentration through a specific attenuation of  $\sigma_{ATN} = 6.5 \text{ m}^2/\text{g}$  (Petzold et al. 2002). Through the use of both transmission and reflectance, Thermo Scientific boasts a truer measurement of aerosol BC. The instrument automatically corrects for temperature and pressure changes of ambient aerosols. The sample line from the inlet to the MAAP was equipped with a sharp cut cyclone to cut out particles larger than  $2.5 \text{ }\mu\text{m}$ . Figure 13 shows the front display of the MAAP.

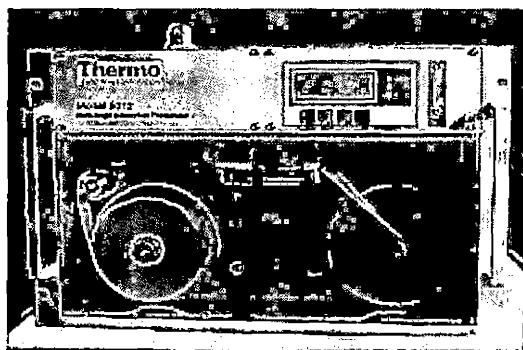


Figure 13. Picture of Multiangle Absorption Photometer

Photoacoustic Extinctionmeter (PAX). The PAX from Droplet Measurements Technology (DMT) (Boulder, Co, USA) is an automated continuous instrument that measures not only BC, but also the extinction coefficient and the single scattering albedo of airborne particles (Figure 14).



Figure 14. Front Display of Photoacoustic Extinctionmeter  
Source: Droplet Measurement Technologies (DMT).  
Photoacoustic Extinctionmeter (PAX).  
<http://www.dropletmeasurement.com/products/ground-based/pax.html> (accessed January 12, 2013)

The instrument produces a continuous real time measurement for in-situ aerosol BC. The PAX does not use a filter media to collect PM, but rather measures the actual in-situ light absorption and scattering of the aerosol PM. A schematic of the PAX instrument can be seen in Figure 15. Light absorption of a particle laden aerosol stream is



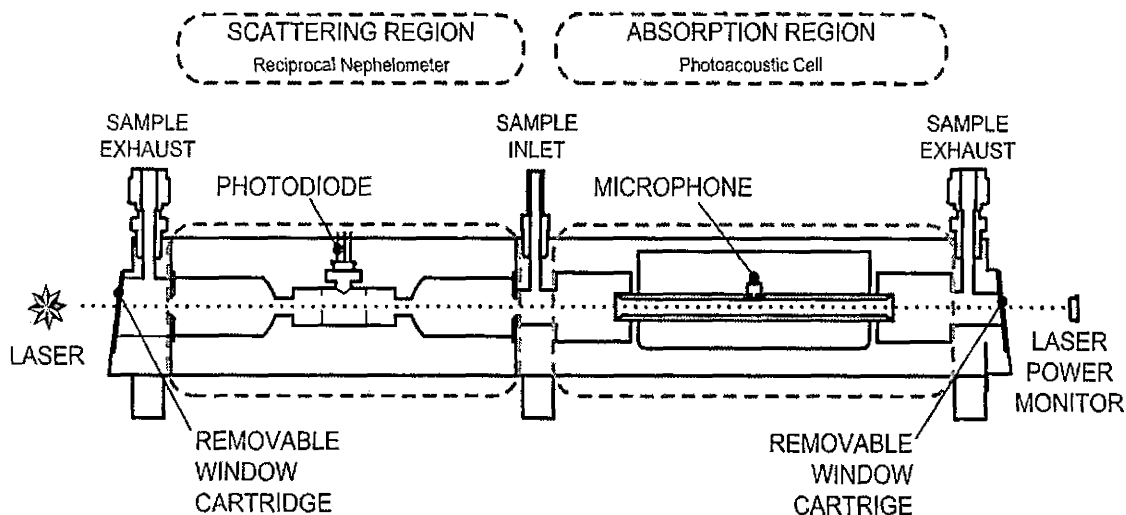


Figure 15. Schematic the Photoacoustic Extinctionmeter  
 Source: Droplet Measurement Technologies(DMT).  
 Photoacoustic Extinctionmeter (PAX).  
<http://www.dropletmeasurement.com/products/ground-based/pax.html> (accessed January 12, 2013)

measured by a sensitive microphone which detects the pressure waves caused by a pulsed laser beam passing through an aerosol with particles absorbing radiant energy and transferring that heat energy to surrounding air and producing pressure waves. The PAX obtains the light scattering coefficient of an aerosol through the use of a wide-angle integrating reciprocal nephelometer. This scattering responds to all particle types regardless of chemical makeup, mixing state, or morphology. The scattering coefficient is a measure of the efficiency of particles to scatter light photons, while the absorption coefficient is

a measure of how many photons are absorbed when light passes through the aerosol. The coefficients are expressed as a number proportional to the amount of photons scattered or absorbed per unit distance (DMT, 2013). The extinction coefficient is the sum of the scattering and absorption coefficients. This value can be utilized to determine the amount of solar radiation that is blocked from reaching the earth' surface (DMT, 2013).

#### Integrated Filter Samples

Integrated 24 hour filter samples were collected by the three Met One Scientific (Grants Pass, OR) SASS units. The SASS units were mounted on the roof of the I-710 air monitoring station as seen in Figure 16. For each day, one

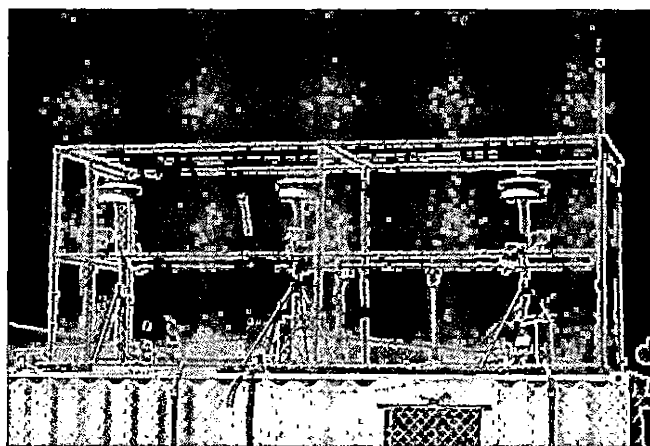


Figure 16. Speciation Air Sampling Systems for Integrated Filter Collection

SASS cartridge with a Teflon filter and another cartridge with a quartz filter was run for 24 hours from 00:00 HR to 24:00 HR. The SASS cartridges were set up with sharp cut cyclones and set to a flow rate of 6.7 L/min. The loaded filters were retrieved from the SASS units and transported to the SCAQMD laboratory within 48 hours after a run date. Teflon filters were stored in a temperature and humidity controlled environment while the quartz filters were stored in a freezer. The Teflon filters were analyzed for BC with a transmissometer while the quartz filters were analyzed for EC with a carbon analyzer.

#### Thermal-Optical Analysis (TOA)

For thermal-optical carbon analysis, several protocols exist within the scientific community. The differences between the protocols involve their temperature profiles time and temperature of steps, purge gas, and method for correcting for the pyrolysis of OC to EC (Schauer et al., 2003). Two commonly used methods are the Interagency Monitoring of Protected Visual Environments (IMPROVE\_A) and the National Institute of Occupational Safety and Health (NIOSH). Three major differences exist between the IMPROVE\_A and NIOSH methods. First, the maximum temperature in the oxygen free environment by which OC is evolved for

IMPROVE\_A is 580°C while the NIOSH method max temperature is 850°C. Secondly, the adjustment for the pyrolysis of OC is calculated through measuring filter reflectance, thermal optical reflectance (TOR), in the IMPROVE\_A method while the NIOSH method measures filter transmittance, thermal optical transmittance (TOT). The third major difference is the point at which the temperature program advances to the next temperature step. The NIOSH method uses fixed residence times at each temperature step while the IMPROVE\_A method advances to the next temperature step when the evolved carbon FID peak returns to a baseline reading (Chow et al., 2001). Table 2 outlines the temperature steps of both the IMPROVE\_A and NIOSH TOA methods.

Table 2. Thermal Optical Analysis Protocols					
Carbon Fraction	Purge Gas	Step	Improve_A (TOR) °C	NIOSH (TOT) °C	Temp Difference °C
OC1	100% HE	1	140	250 (1 min)	110
OC2		2	280	500 (1 min)	220
OC3		3	480	650 (1 min)	170
OC4		4	580	850 (1.5 min)	270
EC1	98% HE 2% O <sub>2</sub>	1	580	650 (0.5 min)	70
EC2		2	740	750 (0.5 min)	10
EC3		3	840	850 (1 min)	10
EC4		4	---	940 (2 min)	

The OC/EC laboratory analyzer utilized in this study was a DRI model 2001 carbon analyzer (Atmoslytic Inc., Calabasas, CA) as seen in Figure 17. The quartz fiber filters (Pall 2500 QAT-UP) were collected daily by the SASS instruments. These filters were analyzed for OC and EC concentrations using TOR as set forth by the IMPROVE\_A protocol. This method quantifies both OC and EC by which total carbon (TC) can be calculated with the sum of the two carbon quantities.

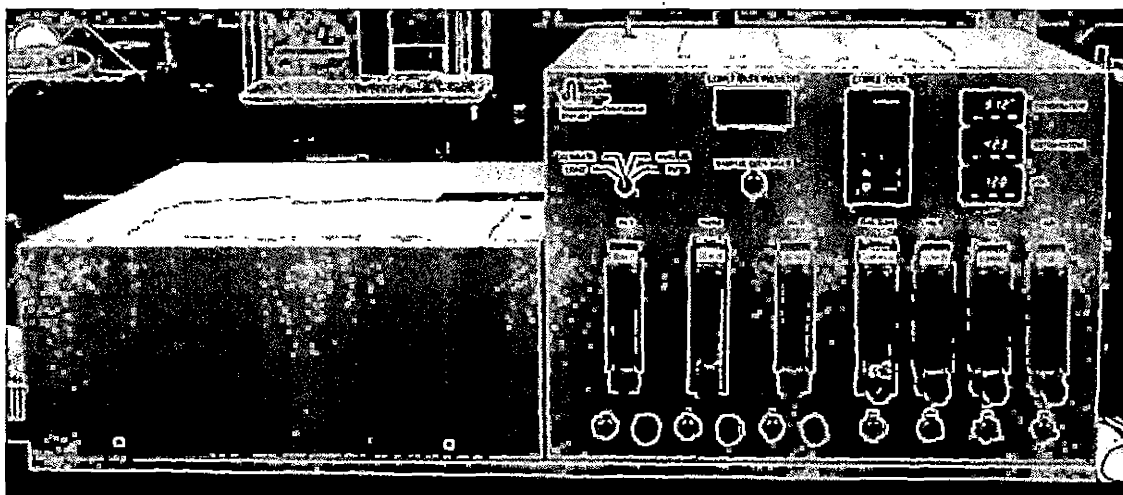


Figure 17. Desert Research Institute Model 2001 Carbon Analyzer

A  $0.502 \text{ cm}^2$  punched portion of a 24 hour integrated quartz filter was placed into a chamber and heated through

a sequence of temperature steps in the presence of one or more purge gases. The split between OC and EC is mostly a function of the temperature protocol used for the analysis, typically NIOSH or IMROVE (Chow et al., 2001; Bae, et al., 2009). OC is defined as that which evolves in a heating cycle under the presence of Helium. EC is defined as that which evolves at a higher temperature with a purge gas containing oxygen (Bae et al., 2004; NIOSH, 1996). The evolved carbon compounds are converted to carbon dioxide ( $\text{CO}_2$ ) by passing through heated manganese dioxide ( $\text{MnO}_2$ ) which acts as an oxidizer. The  $\text{CO}_2$  is then reduced to methane ( $\text{CH}_4$ ) by passing through a hydrogen-enriched nickel catalyst acting as a methanator (Chow et al., 2004). A schematic of the DRI thermal/optical carbon analyzer can be seen in Figure 18. The  $\text{CH}_4$  is then quantified by a flame ionization detector (FID).

Under the pure helium gas steps to evolve OC from the filter, some OC is converted to EC as a result of thermal decomposition. The pyrolysis of OC to EC is often referred to as charring. This pyrolyzed OC will be reported as EC if not properly accounted for as OC. The IMPROVE\_A method corrects for the pyrolysis of OC to EC through continuously monitoring the filter reflectance throughout the OC/EC

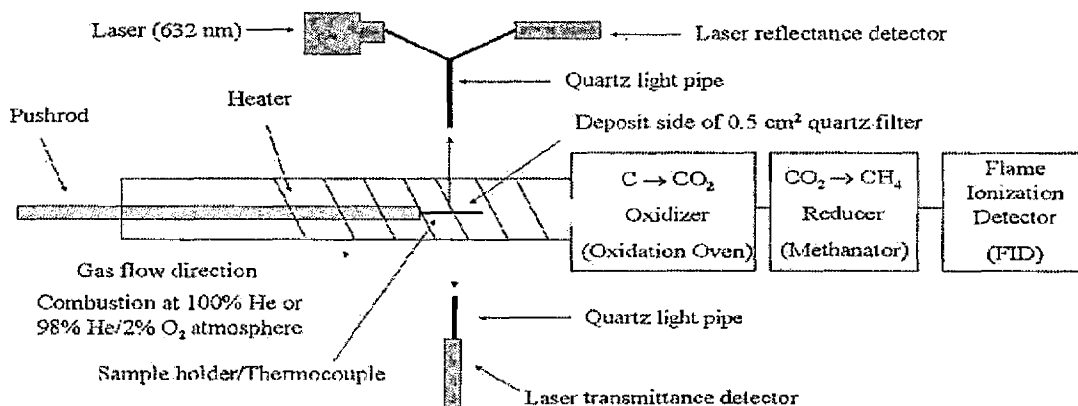


Figure 18. Schematic of Desert Research Institute Carbon Analyzer

Source: Chow, J.; Watson, J.; Chen, L.; Arnott, W.; Moosmuller, H. Equivalence of Elemental Carbon by Thermal/optical Reflectance and Transmittance with Different Temperature Protocols. *Environ. Sci. Technol.* 2004, 38(16), 4414-4422.

analysis. The filter reflectance is dominated by the presence of light absorbing carbon and will therefore decrease during pyrolysis and increase as light absorbing carbon evolves from the filter. The portion of the EC peak due to pyrolysis of OC can be attributed back to OC by monitoring filter reflectance. The portion between the point when He switches to He/O<sub>2</sub> and reflectance returns to its original value is the amount of EC attributed to OC charring. Since OC is typically 10 times more abundant than

EC, a small percentage bias in OC may result in a very large percentage bias for EC (Andreae and Gelencsér, 2006).

Each sample was analyzed in duplicate to ensure reproducibility of the results. When TC was greater than 5  $\mu\text{g}/\text{cm}^2$ , a valid replicate result for TC, OC, and EC must be within  $\pm 15\%$  of the first analysis. If TC was less than 5  $\mu\text{g}/\text{cm}^2$ , then a valid replicate analysis for TC, OC, and EC must be with  $\pm 0.75 \mu\text{g}/\text{cm}^2$  of the first results for TC, OC, and EC. When the above criterion was not met for the first two filter sample analyses, additional filter punches were analyzed until two of the results met the duplicate criteria. Each sample was internally calibrated with a 5% methane standard. For every analysis, the calibration peak area of the internal methane standard was with 95% to 105% of the average calibration peak area for the day.

Light Transmission Method (LTM). An Optical Transmissometer (OT-21) manufactured by Magee Scientific (Figure 19) was used to determine the BC concentration of 24 hour integrated Teflon filters. The Teflon filters were 47 mm filters from supplied through the USEPA for the Federal Reference Method for determining  $\text{PM}_{2.5}$  mass.

The transmissometer is outfitted with a movable dual filter tray. The inner filter is a reference blank and the



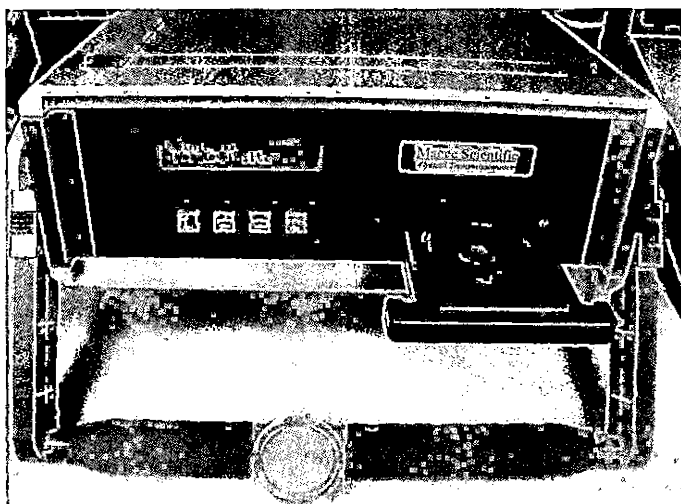


Figure 19. Magee Scientific Optical Transmissometer

outer filter holds the particle laden filter to be analyzed for BC. Both the reference blank Teflon filter and the loaded filter were backed by a 47mm quartz filter to act as a diffuser in order to render higher readings for accuracy.

The OT-21 is modeled on the optics used in the aethalometers (Ahmed, et al., 2009). The transmission intensity of light at 880 nm for BC and 370 nm for aromatic organic compounds is measured for the reference blank and the loaded filter to determine the ATN.  $ATN = -\ln(T/T_0)$  in which  $T$  and  $T_0$  are transmission intensity of light through the loaded filter and blank filter. The relative ATN is divided by the specific attenuation coefficient ( $\sigma_{ATN}$ ) of  $10.0 \text{ m}^2\text{g}^{-1}$  to obtain BC mass on FRM Teflon filters (Neil et

al., 2009).  $BC = ATN/\sigma_{ATN}$ . The BC mass density can then be converted to BC concentration in  $\mu\text{g}/\text{m}^3$ . When using quartz filters, the  $\sigma_{ATN}$  used to convert ATN to BC mass is same as the legacy aethalometers with  $\sigma_{ATN} = 16.6 \text{ m}^2\text{g}^{-1}$ . However, Teflon filters have different properties than quartz filter in how the particles penetrate the fibers of the filter material and in how the particles are then exposed to an intensity of illumination that is increased by multiple reflections at a microscopic scale within the matrix of fibers (Hansen, personal communication). The time of analysis for one filter is typically less than thirty seconds to obtain results for optical attenuation. This method provides a non-destructive means to determine BC quickly.

A neutral density photometric standard filter kit was used to verify instrument calibration and validate the photometric response at the beginning and end of analyzing the FRM Teflon filters. The photometric standard filter kit is equipped with glass standards ranging from light to dark with known and stable optical absorptions. These neutral density filters are traceable reference standards.

Each sample was analyzed two times on the transmissometer. Every ten samples, the blank sample was

checked and a duplicate sample of the prior ten samples was reanalyzed to validate instrument response over time.

#### Complementary Data

Data for meteorological conditions was recorded throughout the instrument comparison study. A RM Young mechanical wind sensor accounted for wind direction and wind speed. Relative humidity along with inside and outside temperature was recorded throughout the study. Traffic data was obtained from the CA Department of Transportation Performance Measurement System which can tracks total vehicle and truck counts along the I-710 corridor (<http://pems.dot.ca.gov>).

#### Statistical Analysis of the Data

Linear regression statistics was performed to determine the degree of correlation between the different measurement methods. Slope and  $R^2$  values provided insights into the observed differences between EC and BC measurements. The results of this data analysis will help investigate the assumptions utilized to convert a signal to BC or EC concentrations, and the effect of time averaging on the observed EC-BC differences.

## Quality Assurance and Quality Control

To assure the quality of the collected data, several measures were initiated for quality assurance and quality control. For continuous instrumentation, flow checks at the beginning, middle, and end of the study were performed. The actual flow through an instrument was measured by utilizing an external standard. The external standard to measure flow was either a BGI Tetra-Cal or a TSI 4140 in-line flow meter. Measuring and recording the actual flow is important to adjust concentration data for actual flow data. For both the AE42 and AE22, the actual flow was on average 3% lower than the instrument displayed flow value. The data from these two aethalometers were then multiplied by 103% to adjust for the flow offset. Similarly, the actual flow for the AE633 was on average 7% less than displayed.

For the integrated 24 hour filter samples, field blanks and three triplicate runs were utilized. For more information on quality assurance and control measures on the analysis of the integrated samples, see the respective methodology sections for the DRI carbon analyzer and Magee Scientific transmissometer.

## CHAPTER FOUR

### RESULTS AND DISCUSSION

The results and discussion portion of this project will be organized similarly to the previous sections. The first portion will examine and compare the results of the continuous instrumentation. The second section will examine the results of the two integrated 24-hour filter methods. The third section will compare the results of the continuous methods to the integrated methods.

#### Continuous Instrumentation

This portion of the results will provide a comparison between continuous BC and EC data. All continuous instruments were operated 24 hours a day for the duration of the study. The timing of the instruments was closely monitored throughout the study in order to properly adjust the data points to the correct timing sequence between instruments. The effect of time averaging on the EC and BC data comparison will be discussed for all continuous instruments. Comparisons between methods will be described through regression statistics. Potential measurement principles that may be influential in creating the observed

differences in EC and BC data will be identified.

Assumptions used to convert a signal into a concentration will be discussed along with other potential causal factors for differences between methods.

Regression statistics involve the slope of the regression line, the intercept of the line, and the  $R^2$  value. The slope is the rate at which the regression line rises when spanning across the horizontal axis. The slope of one method to another yields the factor that method y's results on average increase relative to method x's results. The intercept is the point at which the regression line crosses the y-axis and the value on the x-axis is zero. It is therefore an offset or bias of method y's results relative to method x. In combination ( $y = (\text{slope})x + \text{intercept}$ ) they yield how method y's results vary with respect to method x's results on average. The  $R^2$  symbol represents the coefficient of determination between two variables. The value of  $R^2$  shows how well the variation in y is explained by the variation in x. As  $R^2$  values decrease from one, the probability that the results are correlated decreases similarly. For the purposes of this study,  $R^2 > 0.80$  indicates a strong correlation, and  $R^2 < 0.60$  is considered weak.

### Effects of Averaging Time

The EC/BC correlation is dependent upon the averaging time used to compare the various instruments. A longer time average in theory should produce smoother results with a stronger correlation. The longer averaging time allows for the effects of atmospheric dynamics and processes on aerosol measurements to be compensated for through time. The change in slope, intercept, and  $R^2$  values due to three different averaging times (i.e. 5, 15, and 60-min averages) can be seen in Figure 20 for some of the continuous instruments. The AE42 and AE22 aethalometers, which have identical methodology with near identical results, are averaged together and represented as the Legacy aethalometers. MAAP, AE633 aethalometer, and PAX data were also included in this comparison.

Strong correlations between the continuous instruments are seen at the 5-min averaging time level with  $R^2$  values ranging from 0.85 to 0.93. These correlation values are surprisingly strong for a 5-min averaging time between continuous instruments. When the averaging time is increased from 5 to 15-min, the range of  $R^2$  values increases to 0.93 - 0.96. As expected, the strongest  $R^2$  values are

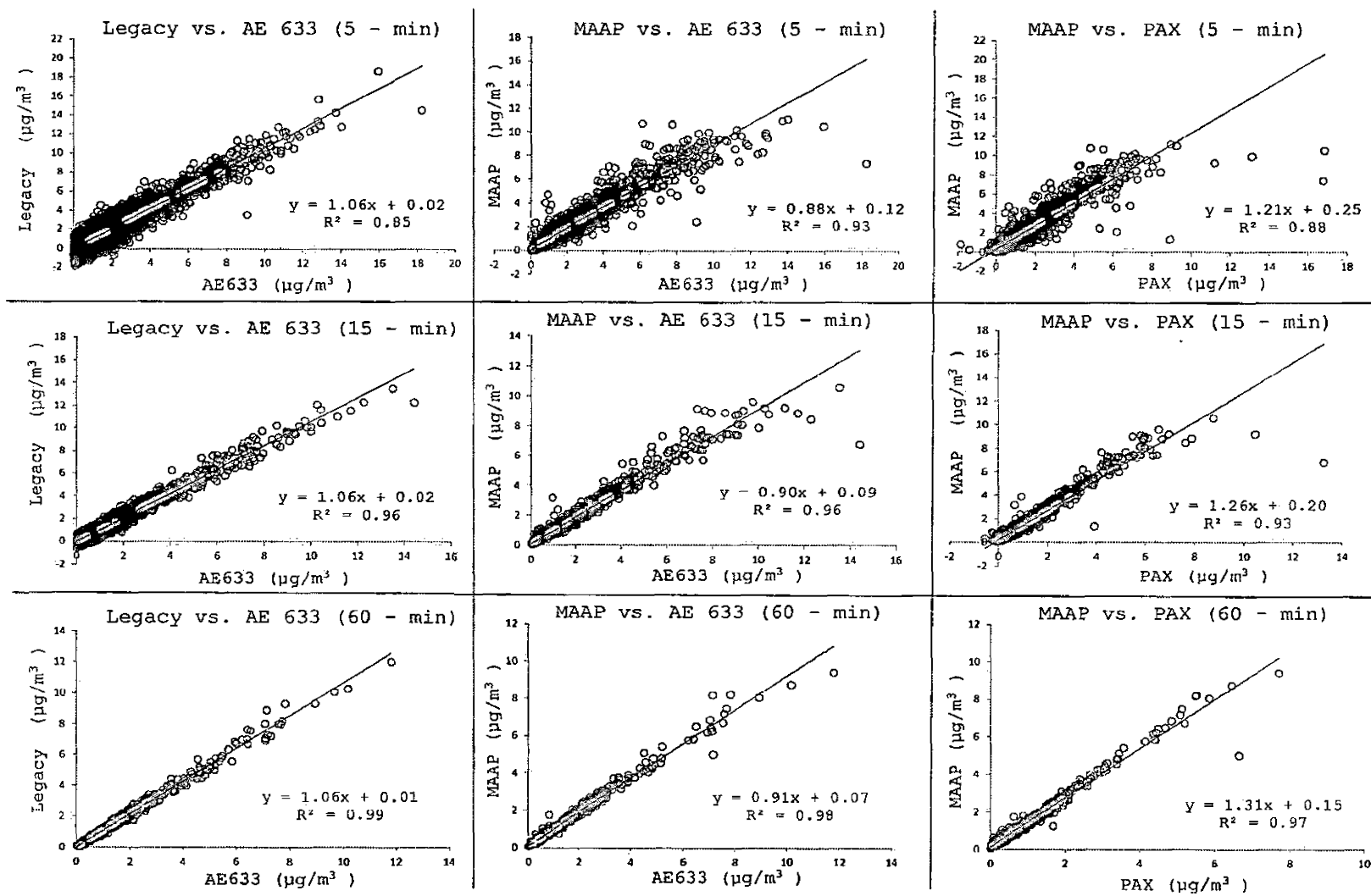


Figure 20. Effects of Averaging Time on Instrument Comparisons



observed for correlations between hourly averages (varied from 0.97 to 0.99).

Linearity is also dependent on averaging time. Some of the results deviate from linearity at high concentrations values, which is most notable at the short 5-min averaging time. Prior studies (Frank et al., 2009) show similar reductions in linearity between BC/EC methods at concentration greater than  $5\mu\text{g}/\text{m}^3$ . The legacy aethalometer and the AE633 aethalometer display good linearity at high concentrations even for 5-min average data. The MAAP and AE633 depict a significant deviation from linearity at high concentrations with the 5-min and 15-min averaging time. With a 60-min average time, the MAAP and AE633 comparison chart shows only slight deviation from linearity at higher concentrations. The slope increases from 0.88 to 0.91 with increasing averaging time from 5-min to 60-min. The MAAP and the PAX also have a significant deviation from linearity at 5-min time resolution and high concentration.

The y intercept values decrease as the averaging time increases. This can be most notably seen with the comparison between the MAAP and PAX. The intercept decreases from  $0.25\mu\text{g}/\text{m}^3$  at 5-min to  $0.20\mu\text{g}/\text{m}^3$  at 15-min and to  $0.15\mu\text{g}/\text{m}^3$  at 60-min averaging time. The intercept

values show the MAAP to be higher than both the AE633 and the PAX at low concentrations. However, the linearity deviation between the MAAP and these instruments shows the MAAP to be lower at high concentrations.

#### Instrument Comparison

The comparability between the continuous BC and EC methods is analyzed in further detail focusing on the averaging time of 1-hr, which is typically used to report most air quality data. Figure 21 shows that all continuous methods track well with one another. In examining Figure 21, the AE22 and AE42 aethalometers (represented by the green and blue lines, respectively) can be visually seen to produce higher BC concentrations. The green and blue peaks are closely followed by the red line representing the AE633.

BC and EC methods can also be compared through regression analyses. The x-axis, which is usually reserved for the independent variable, is chosen arbitrarily in these comparisons since no known reference method for BC or EC exists. Regression statistics are used to understand how well the BC or EC concentrations of one method can be predicted by knowing the concentrations of another BC or EC method.

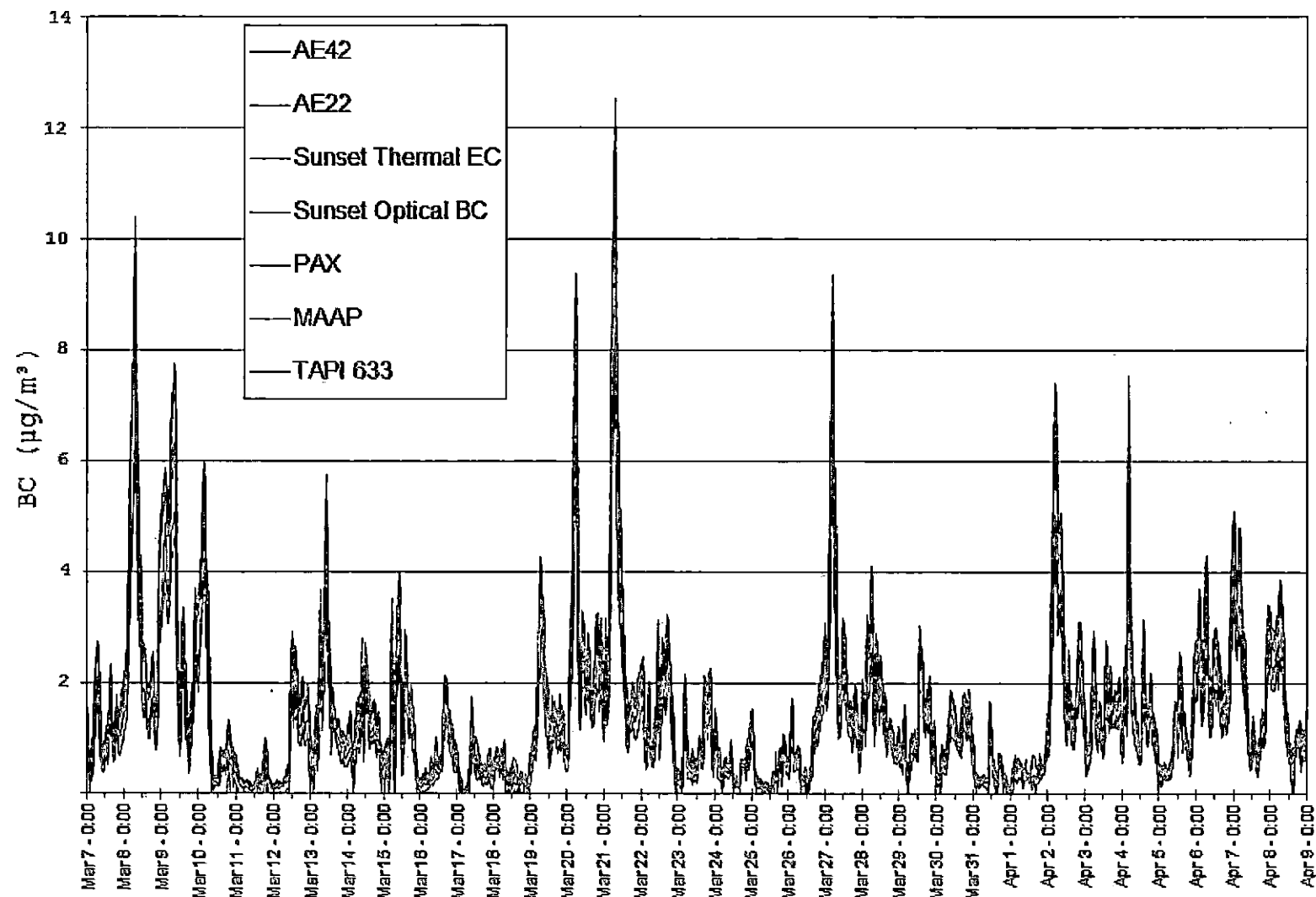


Figure 21. Comparison of Continuous Methods

### Regression Analysis Trends

Table 3 summarizes the  $R^2$  values while Table 4 is a summary of the regression slopes and Table 5 is a summary of the intercept values between the continuous methods with an averaging time of 1-hour. The slope values between the continuous methods range from 0.74 to 1.52. The  $R^2$  values are all greater than 0.94 which shows a high correlation between all the continuous instruments at the 1-hour averaging time. The intercept values for the continuous methods with a 1-hour averaging time range from -0.08 to 0.14  $\mu\text{g}/\text{m}^3$ . In looking strictly at optical based continuous methods, the range of  $R^2$  values is slightly higher ranging from 0.96 to 0.99. When measurements are highly correlated ( $R^2$  close to 1) but have slopes that differ from unity, the results from the continuous instruments differ from one another by a standard percentage or amount which is consistent across high and low concentrations. These variations can be described as systematic in nature and are probably related to the assumptions made to convert the measurement signals of the various instruments into actual BC concentrations.

Table 3. R-Squared Values between Continuous Methods (1-hr Averaging Time)					
	AE633 BC	Legacy Aeths BC	Sunset Thermal EC	Sunset Optical BC	PAX BC
AE633 BC					
Legacy Aeths BC	0.99				
Thermal EC	0.95	0.95			
Optical EC	0.96	0.98	0.94		
PAX	0.98	0.98	0.95	0.96	
MAAP	0.98	0.99	0.95	0.98	0.97

Table 4. Slopes Values between Continuous Methods (1-hr Averaging Time)						
	AE633 BC	Legacy Aeths BC	Sunset Thermal EC	Sunset Optical BC	PAX BC	<b>Y axis</b>
AE633 BC						
Legacy Aeths BC	0.93					
Sunset Thermal EC	1.26	1.34				
Sunset Optical BC	1.26	1.32	0.96			
PAX BC	1.43	1.52	1.09	1.13		
MAAP BC	1.07	1.15	0.78	0.89	0.74	
<b>X axis</b>						

Table 5. Intercept Values between Continuous Methods (1-hr Averaging Time) ( $\mu\text{g}/\text{m}^3$ )						
	AE633 BC	Legacy Aeths BC	Sunset Thermal EC	Sunset Optical BC	PAX BC	<b>Y axis</b>
AE633 BC						
Legacy Aeths BC	0.01					
Sunset Thermal EC	0.14	0.14				
Sunset Optical BC	0.01	0.01	-0.05			
PAX BC	0.10	0.12	0.03	0.10		
MAAP BC	-0.04	-0.05	-0.02	-0.05	-0.08	
<b>X axis</b>						

#### Legacy Aethalometers

The AE22 and AE42 aethalometers are built by the same manufacturer (Magee Scientific) and measure BC under the same methodology. The two instruments correlate very well with a regression equation of  $y = 1.03x - 0.03$  with an  $R^2 = 0.99$ . The regression scatter plot between these two aethalometers can be seen in Figure 22. Since these two instruments have the same analytical performance and

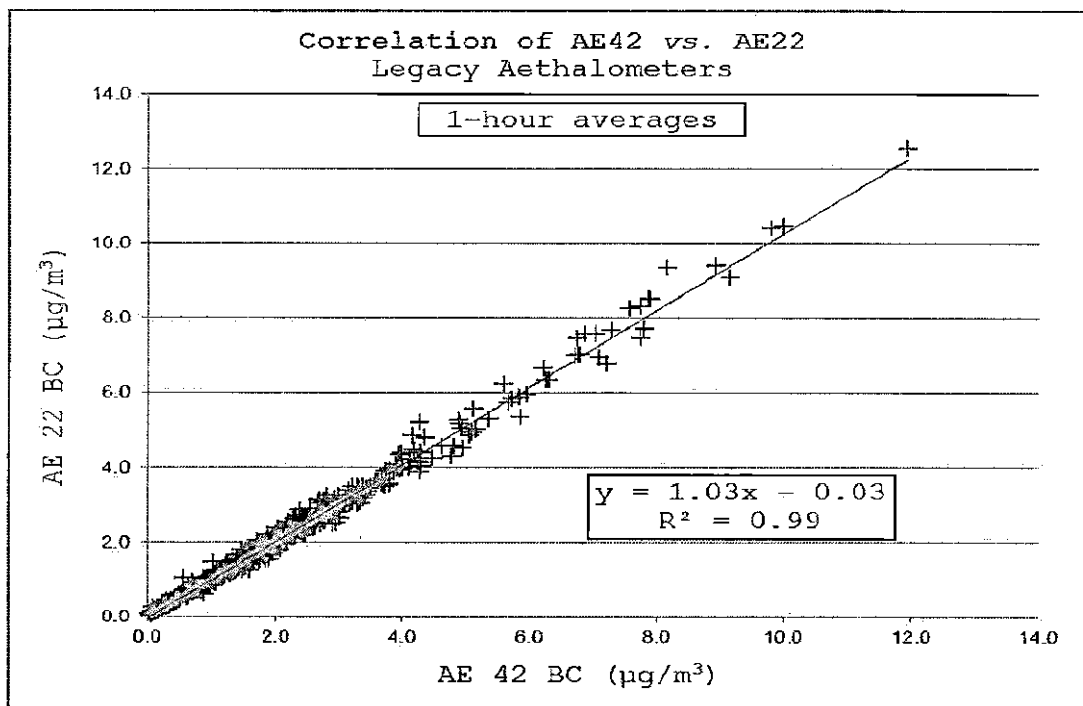


Figure 22. Correlation of Legacy Aethalometers

instrument methodology, the two are averaged together and labeled as the Legacy Aethalometers. The slope values in Table 4 comparing the Legacy Aethalometers to other continuous methods indicate that the BC concentrations from the legacy aethalometers are greater than the other continuous methods.

#### Legacy and Dual Spot Aethalometer

The new dual spot aethalometer correlates well with the older legacy aethalometer. Differences in analytical performance are expected between the two BC instruments as

the new aethalometer has been upgraded to correct for spot loading effects. With the legacy aethalometers as the x-axis and the AE633 on the y-axis, the regression line for one hour averages has a slope of 0.93, intercept of 0.01  $\mu\text{g}/\text{m}^3$ , and an  $R^2 = 0.99$  (Figure 23).

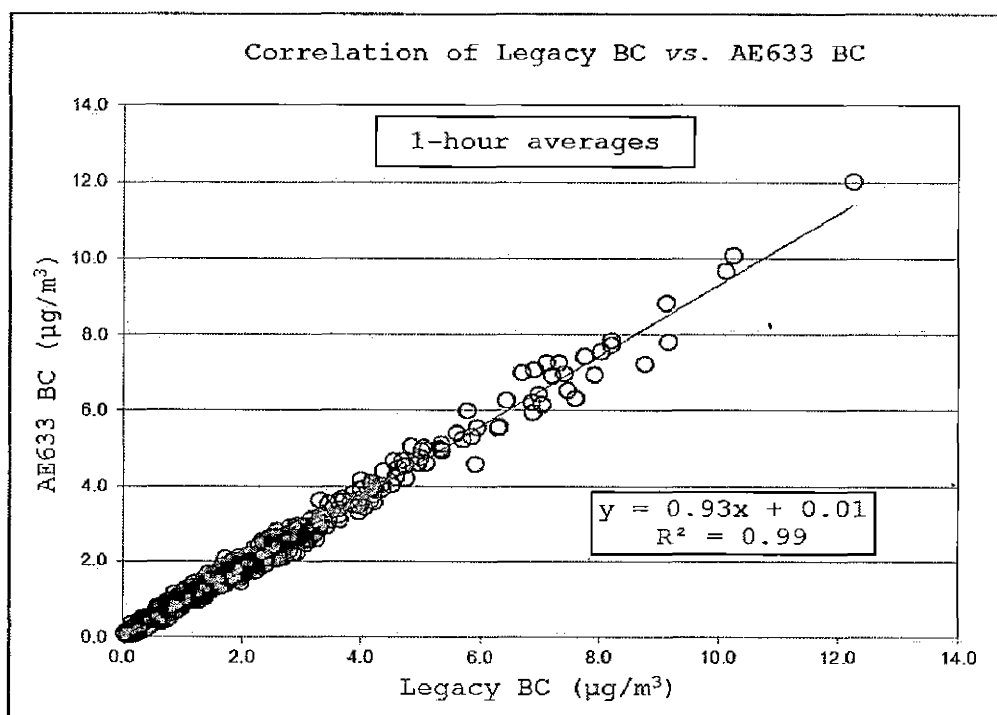


Figure 23. Correlation of Legacy and Dual Spot Aethalometer

The BC concentrations for the 633 are lower than the legacy aethalometers BC. Several factors may be influential in creating the differences between the instruments. The wavelength of the light source utilized by the two



instruments is the same at 880nm (infrared spectrum). The AE633 is able to measure ATN at up to 10 different wavelengths; however in comparison with other BC and EC instruments, the wavelength of 880nm is used to determine BC. The two instruments utilize different types of tape media with the legacy instruments using a quartz fiber filter and the AE633 using a T60 Teflon glass fiber filter.

Spot loading effects occur when collected particles in the filter matrix cause a shadowing effect which can be visually seen in Figure 24 for BC concentrations greater than  $0.2 \mu\text{g}/\text{m}^3$ .

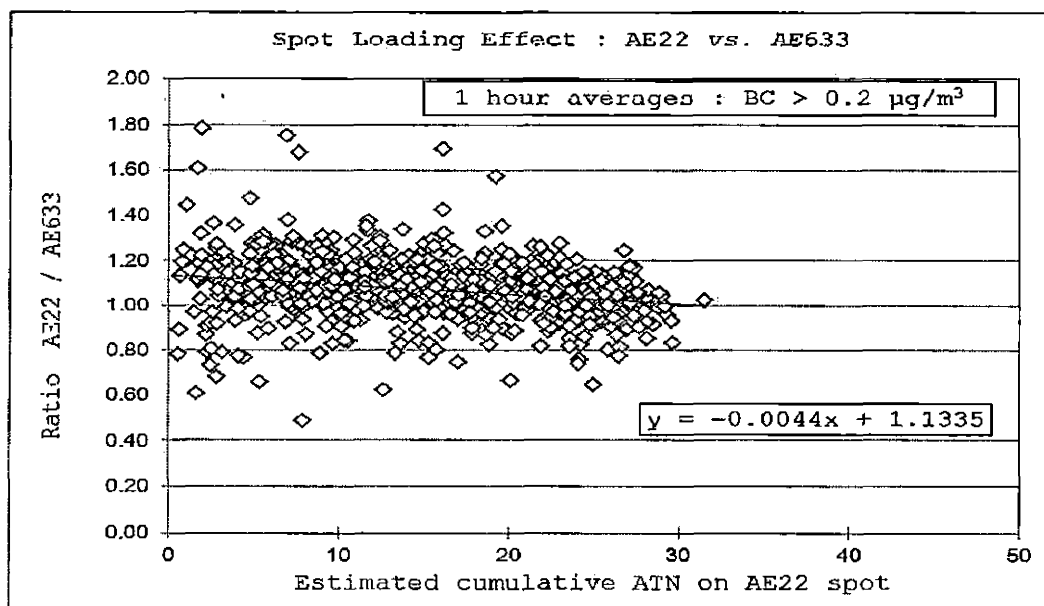


Figure 24. Spot Loading Effect: Aethalometers

This shadowing effect causes the instrument to underestimate the absorption coefficient. The ratio of AE22 BC divided by AE633 BC plotted against the estimated cumulative ATN on the AE22 filter spot provides an indication the filter loading effect on the AE22. The cumulative ATN would be low right after a tape spot change and would be high just before a tape spot change.

#### Aethalometers to Multiple Angle Absorption Photometer

For 1-hour averages, BC concentrations obtained by the MAAP were found to be lower than the legacy aethalometer BC concentrations. The slope between the two methods with the legacy aethalometers as the y-axis is 1.15 and the intercept is  $-0.05 \mu\text{g}/\text{m}^3$ . The correlation coefficient between the methods is  $R^2 = 0.99$ . The slope difference is assumed to be systematic in nature with the high correlation coefficient at 0.99 indicating the difference to be consistent across high and low concentration. The Legacy Aethalometer and the MAAP instruments have different optical geometry, filter media, and conversion factors to convert ATN to BC mass.

The Thermo Scientific MAAP and the AE633 aethalometer correlate very well with a slope of 1.07, intercept of -

0.04  $\mu\text{g}/\text{m}^3$ , and an  $R^2 = 0.98$ . The correlation between the MAAP and AE633 can be seen in Figure 25.

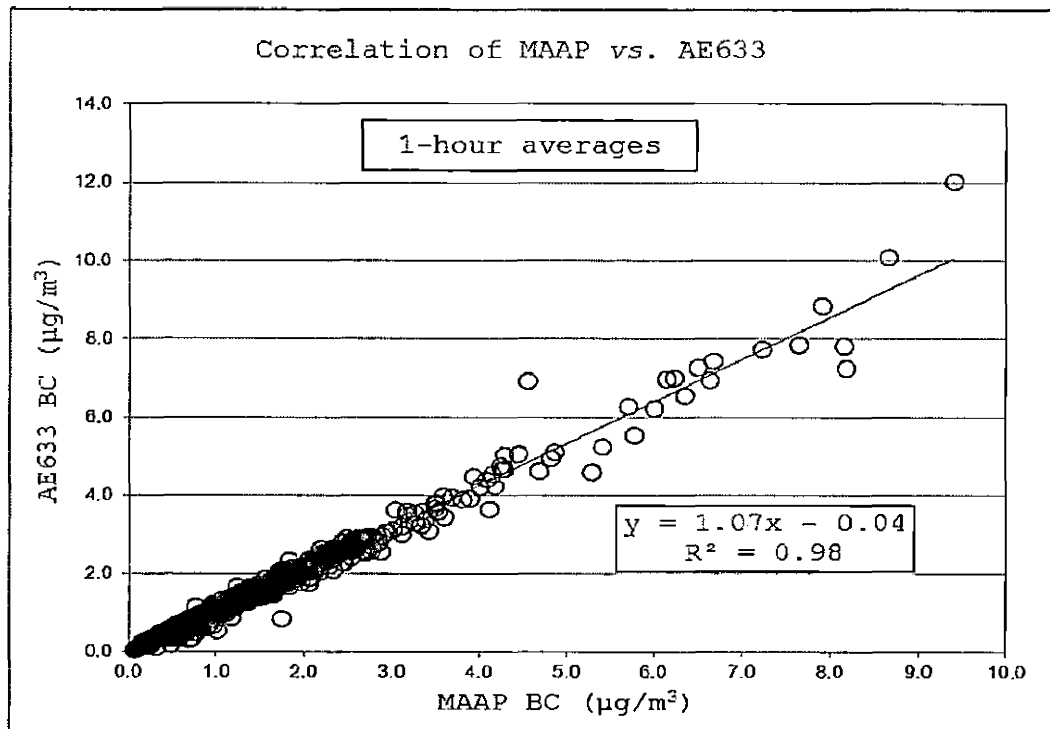


Figure 25. Correlation of Multiple Angle Absorption Photometer and Dual Spot Aethalometer

The new dual spot aethalometer on average provides slightly higher BC results than the MAAP. Both of these methods are optical filter based methods for determining BC. However, the measurement principles of these two methods differ significantly with the filter tape used for collecting PM, wavelength of light source, correction

factors for filter artifacts, and conversion factors for converting ATN to BC mass. The MAAP uses a glass fiber filter with a light source at 660nm while the AE633 uses a T60 Teflon glass fiber filter with a light source at 880nm. The methodology to convert an optical signal into a concentration for both of these instruments involve real-time continuous corrections for problems associated with obtaining BC measurements from optical filter based methods. Many of the filter based real time BC monitors have shown a dependence on the loading of PM on the filter matrix. The causal factors for a non 1:1 relationship between the MAAP and AE633 may lie in the automatic correction methods used to compensate for the dependence on filter loading and aerosol scattering effects. The geometry of the optics between these instruments differs significantly with the aethalometer using transmittance to obtain optical attenuation while the MAAP uses both transmittance and reflectance at multiple angles to compensate for potential filter artifacts. Based on the MAAP's measurement principle of observing both transmittance and reflectance with multiple detectors, Thermo Scientific claims the MAAP does not need a correction for either filter loading or aerosol scattering

effects based on the 2002 Reno Aerosol Optical Study (Jernigan and Goohs, 2006; Sheridan et al., 2005). The dual spot technology aethalometer measurement with two sampling chambers at different flow rates allows the instrument to correct the actual BC measurements for the filter loading effect.

#### Sunset Carbon Analyzer to Aethalometers and Multiple Angle Absorption Photometer

The legacy aethalometers BC concentrations for 1-hour averages is higher than both the Sunset optical BC and Sunset thermal EC concentrations. The slope with the legacy aethalometers on the y axis is 1.34 in comparison to Sunset thermal EC and 1.32 in comparison to Sunset optical BC. The  $R^2$  value between the legacy and Sunset thermal EC is 0.95 and between the legacy and Sunset optical BC is 0.98. The intercept value between the Legacy Aethalometers and Thermal EC is  $0.14 \mu\text{g}/\text{m}^3$  while the intercept between the Legacy and the optical BC measurement is lower at  $0.01 \mu\text{g}/\text{m}^3$ .

The AE633 one hour average BC concentrations were also found to be higher than both the Sunset optical BC and Sunset thermal EC. With the AE633 on the y axis, the slope is 1.26 for both the Sunset thermal EC and optical BC. The

$R^2$  value for the regression between the AE633 and Sunset thermal EC is 0.95 and between the AE633 and Sunset optical BC is 0.96. The intercept value between the AE633 and Thermal EC is  $0.14 \mu\text{g}/\text{m}^3$  while the intercept between the AE633 and the optical BC measurement is much less at  $0.01 \mu\text{g}/\text{m}^3$ .

The MAAP for one hour average BC concentration is higher than both the Sunset thermal EC and optical BC concentrations. The regression slope between the two methods with the MAAP as the x axis is 0.78 with the Sunset thermal EC and 0.89 with the Sunset optical BC. The regression coefficient with the MAAP to Thermal EC is 0.95 and with the MAAP to Sunset optical BC is 0.98. The comparison between the two Sunset methods and the MAP can be seen in Figure 26.

The aethalometers and the MAAP correlates better with the Sunset optical BC measurement than the thermal EC measurement. This is expected as the aethalometers, MAAP, and Sunset optical BC are measurements based on the optical properties of carbonaceous PM, while thermal EC is measuring a different methodologically defined species. Other potential causes for slope variation include the differences in wavelength of the light source, filter

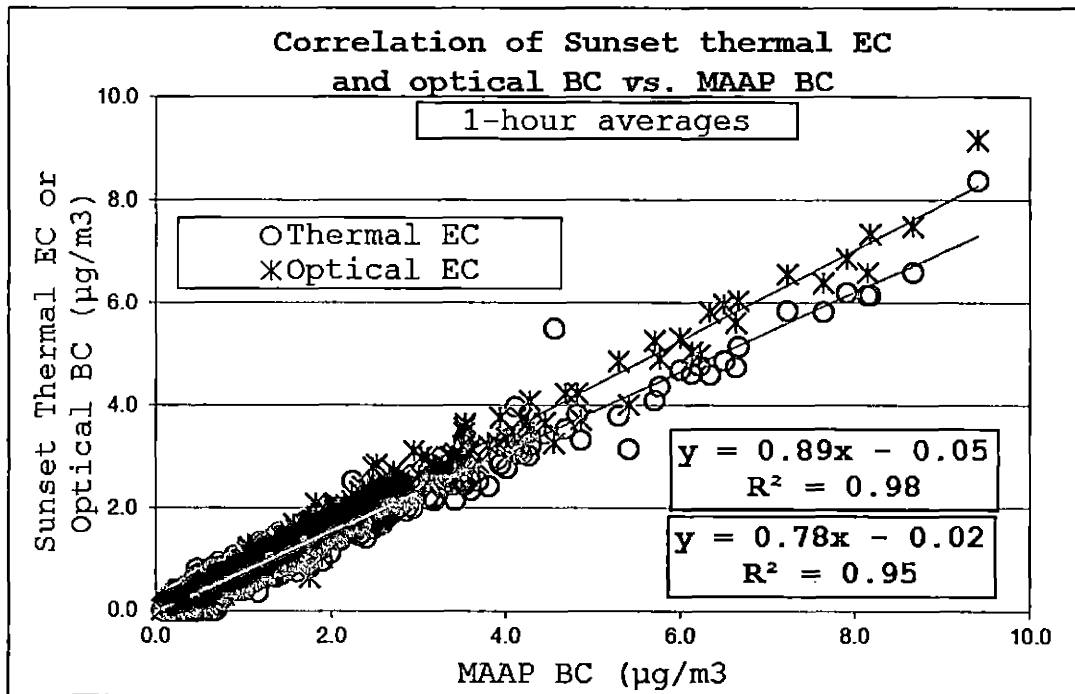


Figure 26. Correlation of Sunset Carbon Analyzer to Multiple Angle Absorption Photometer

media, optical geometry, and conversion factors for converting ATN to BC mass.

#### Sunset Optical BC to Sunset Thermal EC

The Sunset semi-continuous carbon analyzer produces hourly thermal EC and optical BC concentrations. The two concentrations are very close in agreement with a regression slope of 0.96 with the Sunset optical method chosen for the x axis. The optical BC concentration is slightly higher than the thermal EC concentration. The correlation coefficient between the two methods is 0.94

which indicates a strong correlation. The strong correlation is expected as the  $\sigma_{\text{ATN}}$  to convert ATN to BC mass for optical BC is dependent on the absorbance and thermal EC measurement.

#### Sunset Thermal EC to Continuous BC Methods

The Sunset laboratory thermal EC measurement correlates well with the continuous measurements for BC. The  $R^2$  values range from 0.94 to 0.95 in comparing to the continuous BC methods. These  $R^2$  values show good correlation, but are the lowest when comparing to the other BC continuous methods. The slopes with thermal EC as the y-axis to the other instruments range from 0.78 to 1.34. The intercepts range from -0.05 to 0.14  $\mu\text{g}/\text{m}^3$ . The Sunset carbon analyzer is the only continuous instrument measuring EC based on the refractory and optical properties of carbonaceous PM. The other continuous methods only measure the optical properties of carbonaceous PM.

#### Photoacoustic Extinctionmeter to other BC Methods

On average, the PAX provides a lower BC concentration than all the other EC/BC continuous methods. The PAX is the only instrument in this comparison study that measures the actual absorption of light of aerosol PM. This in-situ measurement is not susceptible to filter artifacts that



affect the various filter based instruments. The PAX is strongly correlated with all the continuous BC/EC methods with an averaging time of 1-hour with  $R^2$  values ranging from 0.95 to 0.98. This indicates strong correlation at both high and low concentration values. With respect to slope values, the Sunset thermal EC (y axis) is the closest continuous method to the PAX BC with a slope of 1.09. The regression coefficient between the Sunset Thermal EC and the PAX is 0.95. The Sunset optical BC to PAX BC also has a strong correlation with an  $R^2 = 0.96$  and a regression slope of 1.13 with the Sunset optical as the y axis. The largest difference between all of the continuous methods is between the PAX and the Legacy Aethalometers. With the legacy aethalometers as the y-axis, the slope of the regression is 1.52. The  $R^2$  between the two methods shows a high correlation at 0.98.

For one hour averaging time, the AE633 average BC concentration is higher than the PAX average BC concentrations. The regression slope between the methods with the AE633 on the y axis is 1.43 with an intercept of  $0.10 \mu\text{g}/\text{m}^3$  and an  $R^2$  value of 0.98. The slope value shows a significant difference between the BC concentration values between the two methods while the high  $R^2$  value shows the

difference to be of a systematic nature and consistent from low to high concentrations. The correlation between the two methods can be seen in Figure 27.

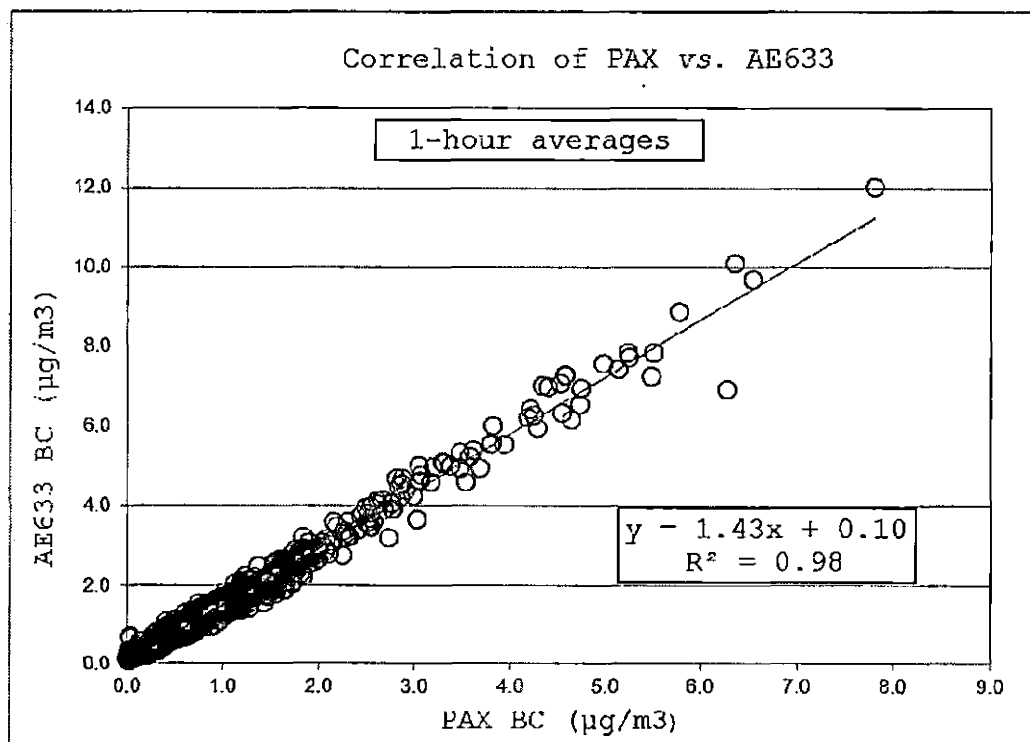


Figure 27. Correlation of Photoacoustic Extinctionmeter and Dual Spot Aethalometer

The filter based optical methods, AE633, Legacy Aethalometers, and the MAAP show strong correlation with the PAX ( $R^2 > 0.97$ ), but with significant slope differences. The filter based optical methods assume that light absorption of particles on a filter is proportional to the

actual particle light absorption. The high correlations between these filter based methods and the PAX indicate that this assumption may be close to reality with some uncertainty between the two measurements. The slope differences between methods may be attributed to the conversion factors used to derive the BC mass from the ATN signal. Understanding the proportional nature between aerosol particle light absorption and filter particle light absorption is essential in obtaining accurate BC measurements from attenuation through a particle laden.

#### Filter Based Continuous Instruments

The difference in BC and EC concentration may be largely influenced by the specific attenuation coefficient used to convert light absorption into mass concentrations. The value of the specific attenuation coefficient is dependent on type of filter media, optical geometry of instrument, emissions source, and wavelength of the light source. The MAAP used a specific attenuation coefficient of  $\sigma_{\text{ATN}} = 6.5 \text{ m}^2/\text{g}$  while the legacy aethalometers use a  $\sigma_{\text{ATN}} = 16.6 \text{ m}^2/\text{g}$ . Many of the optical methods measure particle light absorption at different wavelengths. The dependence of particle light absorption on wavelength must be known or accounted for through the specific attenuation coefficient.

The source of carbonaceous PM may also affect the specific attenuation coefficient. Wood smoke emission sources absorb light differently than other incomplete combustion emissions sources.

Some optical methods correct for spot loading effects and/or light scattering effects which will affect the optical measurement. The filter matrix effects can bias the specific attenuation coefficient both negatively and positively. The shadowing of collected particles in the filter matrix causes the instrument to underestimate the absorption coefficient. The multiple scattering of light by both the filter and aerosol particles causes the instrument to overestimate the absorption coefficient. Other light absorbing particles (e.g. Iron) in the aerosol PM may affect measured EC (Frank et al., 2009).

#### Micro Aethalometers

The micro aethalometers are not ideally designed to be utilized as they were in this study as an ambient air quality station BC monitoring device. These devices are designed to be mobile personal BC monitors that can be worn for a limited period of time. For that reason, the discussion of these instruments will be limited and set apart from the above continuous BC monitoring devices. The

typical length of sampling time per filter was between 48 and 72 hours. Filter loading effects were significant with these instruments as the filter spot location is constant until the filter was changed manually by staff. The regression statistics between the average of the micro aethalometers on the y axis and the legacy aethalometers on the x axis reveal a slope of 0.66, an intercept of 0.17  $\mu\text{g}/\text{m}^3$ , and an  $R^2$  value of 0.89 (Figure 28). The linearity between the methods decreases as at higher concentrations.

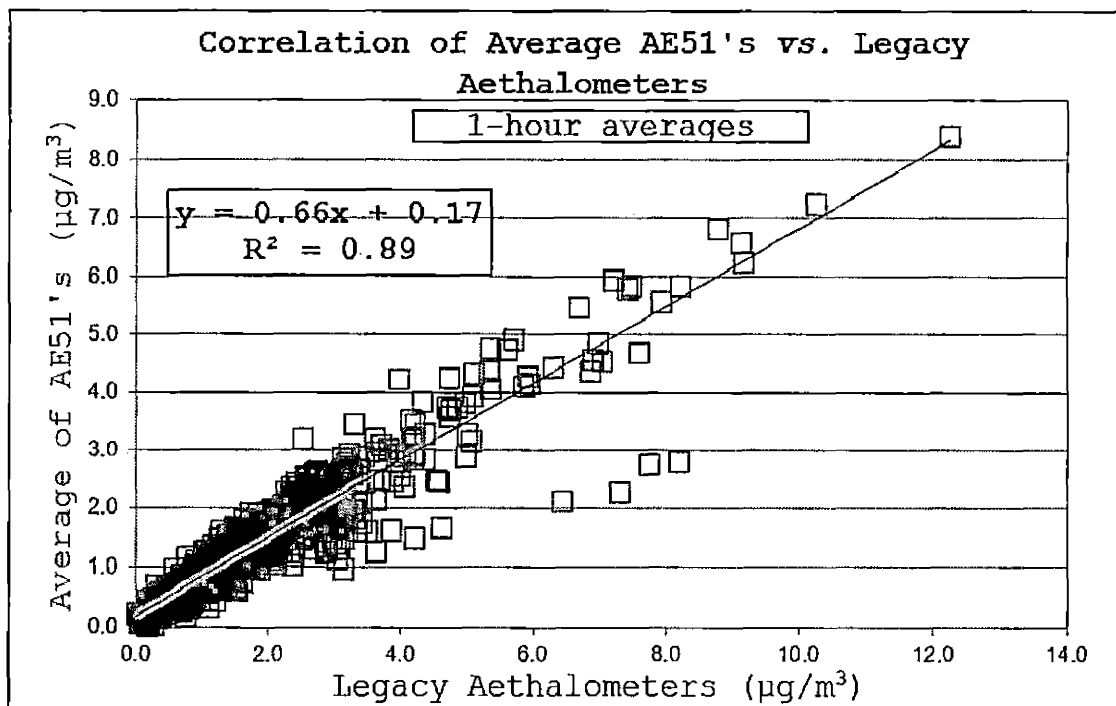


Figure 28. Correlation of Legacy and Micro Aethalometers

### One-minute Data Noise for Aethalometers

March 18, 2012 was a day characterized by high humidity with roughly 0.2 inches of precipitation for the day. This day was chosen to understand the effects of relative humidity (RH) on the legacy aethalometers and the new AE633 aethalometer. Figure 29 shows the difference between the AE633 in red and the legacy aethalometers with respect to changes in RH. The response of the legacy aethalometers was found to be much noisier than the other continuous instruments at the 1-min averaging time.

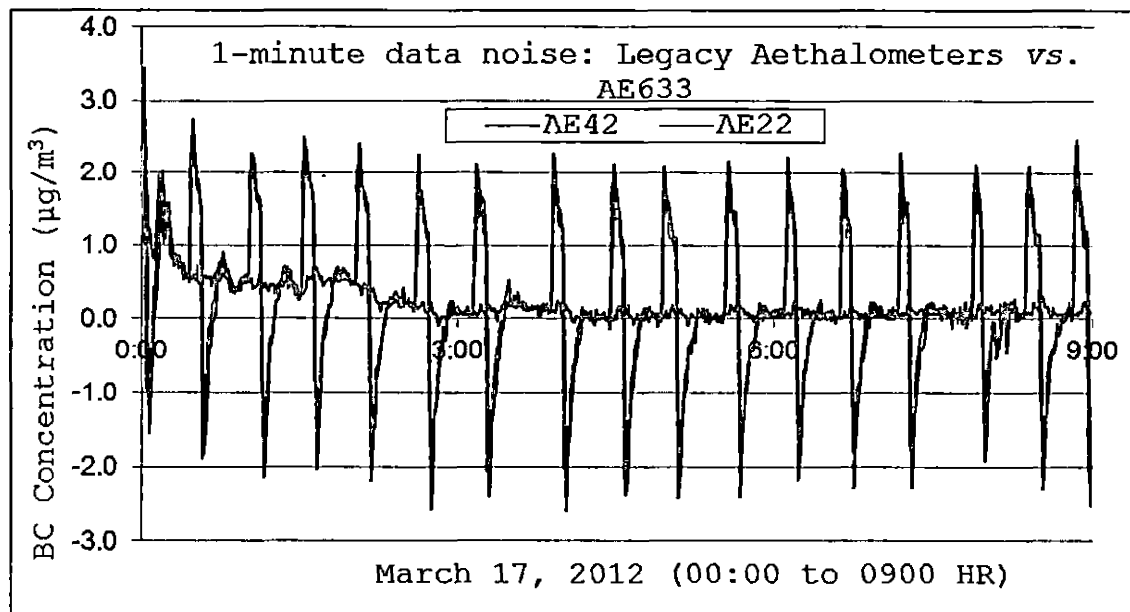


Figure 29. 1-minute Data Noise: Legacy and Dual Spot Aethalometer

As seen in Figure 29, the instrument response at the 1-minute averaging time is characterized by a periodic high spike followed by a low spike. However, it appears that hourly averages are not significantly affected, since the high and the low spikes tend to offset one another. The time-series plot as seen in Figure 29 indicates these fluctuations are potentially caused by the on-off cycling of an air-conditioner. The manufacturer of the aethalometer, Magee Scientific, has indicated the effect is due to variations in RH of air surrounding the equipment and not due to temperature variations. When the RH is moderately high, the air exiting from the air conditioner will have passed over cold refrigeration coils with a substantially lower humidity level than the general surrounding air. The variations in RH create a very small change in the optical properties of the filter material. This, in turn, is interpreted by the algorithm in the aethalometer as an artifact on the data. The artifact is amplified as a result of the instrument operating on a one-minute time-base.

## Integrated 24-hour Filter Methods

The integrated quartz filters were analyzed for thermal EC by the DRI carbon analyzer using the IMPROVE\_A protocol with thermal optical reflectance. The Teflon filters were analyzed for BC using the light transmission methods (LTM) method with a Magee Scientific Transmissometer OT-21.

### Integrated EC to Integrated BC

The comparison between the Integrated EC and Integrated LTM BC is of interest as these are the only integrated 24-hour filter methods in this comparison study. The two methods compare well with one another with a good correlation at  $R^2 = 0.87$ , slope of 1.13, and an intercept of  $0.12 \mu\text{g}/\text{m}^3$  with integrated EC as the x axis. The correlation of these two methods is depicted in Figure 30. The optical LTM is on average greater than integrated thermal EC. The optical properties of the filter analyzed can be affected by the carbonaceous PM source mix (e.g. Wood smoke sources vs. motor-vehicle incomplete combustion sources). In the presence of wood smoke, optical ATN measurements increase creating the need for a larger  $\sigma_{\text{ATN}}$  to convert ATN to BC mass (Neil et al., 2009).



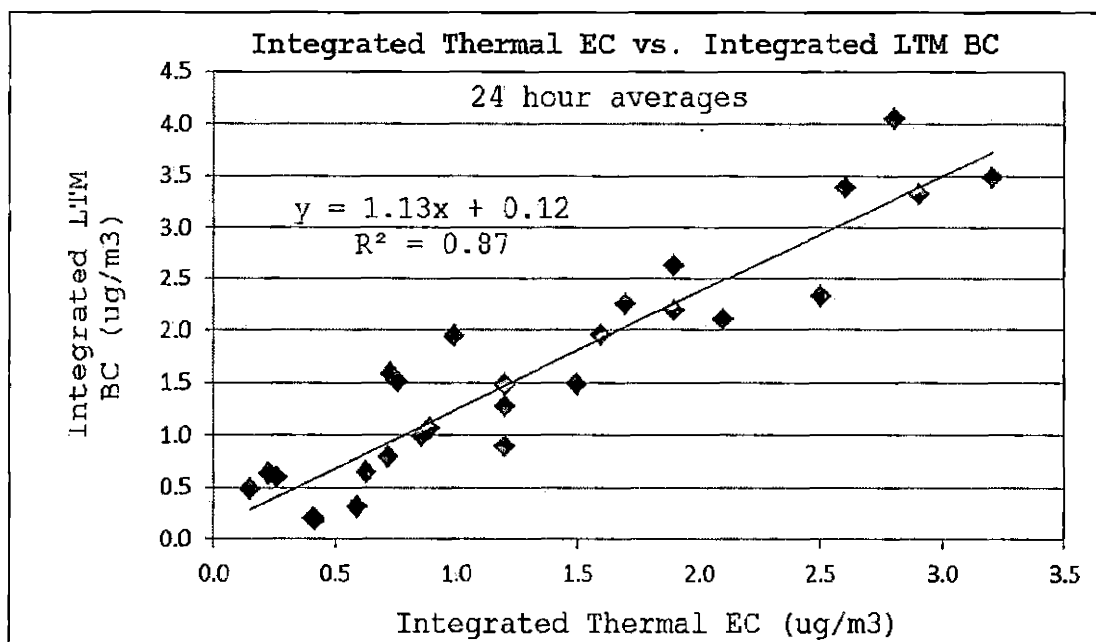


Figure 30. Integrated Elemental Carbon and Integrated Black Carbon

The linearity between the methods is consistent for the range of concentrations found at the I-710 freeway air monitoring station. Non-linearity at concentrations greater than 5 ug/m<sup>3</sup> have been seen in previous studies comparing transmissometer BC and TOA EC (Frank et al., 2009) due to potential saturation effects with increasing concentrations. The optical filter absorption is dependent on wavelength, filter material, and other potential light absorbing aerosols. Iron oxide may also absorb light which would cause an increase in the measured light absorption.

## Integrated 24-hour Filter Methods to Continuous Methods

The averaging time for the continuous instruments was set to 24 hours in order to compare with the 24 hour integrated filter sample analysis. The correlation  $R^2$  values between the methods are displayed in Table 6, the slope values between methods are shown in Table 7, and the intercept values between methods are shown in Table 8.

### Integrated EC

The integrated filter EC determined through TOR IMPROVE\_A protocol correlates well with the continuous methods. The regression statistics for integrated filter EC with the continuous instruments ranges from  $R^2$  of 0.84 to 0.94. The slopes between the integrated EC as the x axis to the continuous instrumentation ranged from 0.76 to 1.17. The intercepts ranged from 0.10 to 0.34  $\mu\text{g}/\text{m}^3$ . In examining the slope relationships between the integrated EC and the continuous instruments, it is evident that the legacy aethalometers, the AE633, and the MAAP BC data are all higher than the corresponding integrated EC values. The legacy aethalometers, AE633, and the MAAP are the three predominantly used continuous optical filter based methods for determining BC.

Table 6. R<sup>2</sup> Values with Averaging Time of 24-hours

	AE633 BC	Legacy BC	Micro AE51 BC	Sunset Thermal EC	Sunset Optical EC	PAX BC	MAAP BC	Integrated EC	y
AE633 BC									
Legacy BC	0.99								
Micro AE51 BC	0.93	0.94							
Thermal EC	0.98	0.98	0.90						
Optical EC	0.98	0.98	0.91	0.96					
PAX BC	0.99	0.99	0.93	0.98	0.98				
MAAP BC	0.99	0.99	0.90	0.97	0.98	0.99			
Integrated EC	0.93	0.94	0.84	0.94	0.94	0.94	0.94		
Integrated LTM BC	0.88	0.88	0.79	0.88	0.88	0.87	0.85	0.87	
x									

Table 7. Slope Values with Averaging Time of 24-hours

	AE633 BC	Legacy BC	Micro AE51 BC	Sunset Thermal EC	Sunset Optical EC	PAX BC	MAAP BC	Integrated EC	y
AE633 BC									
Legacy BC	0.93								
Micro AE51 BC	1.27	1.40							
Thermal EC	1.28	1.38	0.94						
Optical EC	1.25	1.35	0.90	0.95					
PAX BC	1.42	1.52	0.77	1.08	1.11				
MAAP BC	1.06	1.15	0.76	0.77	0.88	0.75			
Integrated EC	1.09	1.17	0.77	0.82	0.86	0.76	1.06		
Integrated LTM BC	0.86	0.94	0.61	0.67	0.69	0.61	0.79	0.77	
x									

Table 8. Intercept Values with Averaging Time of 24-hours ( $\mu\text{g}/\text{m}^3$ )									
	AE633 BC	Legacy BC	Micro AE51 BC	Sunset Thermal EC	Sunset Optical EC	PAX BC	MAAP BC	Integrated EC	Y
AE633 BC									
Legacy BC	0.01								
Micro AE51 BC	-0.09	-0.13							
Sunset Thermal EC	0.10	0.08	0.22						
Sunset Optical EC	-0.01	-0.01	0.17	-0.04					
PAX BC	0.10	0.12	0.24	0.04	0.11				
MAAP BC	-0.03	-0.05	0.15	-0.01	-0.05	-0.09			
Integrated EC	0.22	0.25	0.34	0.16	0.20	0.10	0.19		
Integrated LTM BC	0.29	0.27	0.37	0.15	0.22	0.11	0.29	0.08	
X									

The comparison of the Sunset thermal EC to Integrated EC is also of interest because these are the only two methods in this instrument comparison study determining EC based on its thermal-optical properties. The correlation between these two methods is strong with  $R^2 = 0.94$ . The slope between the two methods with integrated thermal EC as the x axis is 0.82 and the intercept is  $0.16 \mu\text{g}/\text{m}^3$ . The integrated thermal EC concentrations are slightly higher than the Sunset Thermal EC which can be seen in Figure 31.

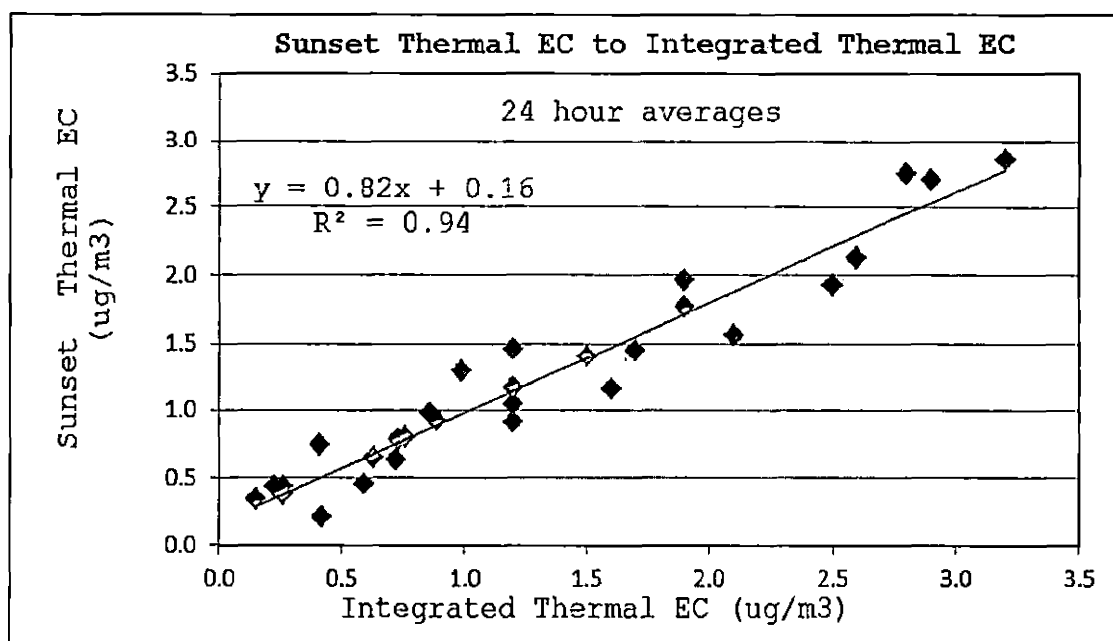


Figure 31. Sunset Carbon Analyzer and Integrated Elemental Carbon

Both of these methods measure EC based on the thermal-optical properties of carbonaceous PM. The slope offset from 1:1 may be a result of differences in the calibration between the two instruments, differences in the two temperature protocols utilized (NIOSH vs. IMPROVE\_A), or differences between the correction methods used to compensate for OC charring (TOT vs. TOR). Typically OC is significantly more abundant than EC, so a small bias in OC may result in a large bias for EC (Andreae and Gelencsér, 2006).

#### Integrated BC

The integrated filter BC determined with the LTM via the OT-21 Magee Scientific transmissometer correlates well with the continuous methods with  $R^2$  values ranging from 0.79 to 0.88. The slopes between the integrated BC as the x axis to the continuous instrumentation ranged from 0.61 to 0.94 and the intercepts ranged from 0.08 to 0.37  $\mu\text{g}/\text{m}^3$ . The transmissometer optical methodology is modeled after the optics used in the aethalometers. The best comparison between the Integrated LTM BC and a continuous method is with the legacy aethalometers with a slope of 0.94, an  $R^2$  value of 0.88, and an intercept of 0.27  $\mu\text{g}/\text{m}^3$  (Figure 32). The LTM integrated BC measurements are higher than all the

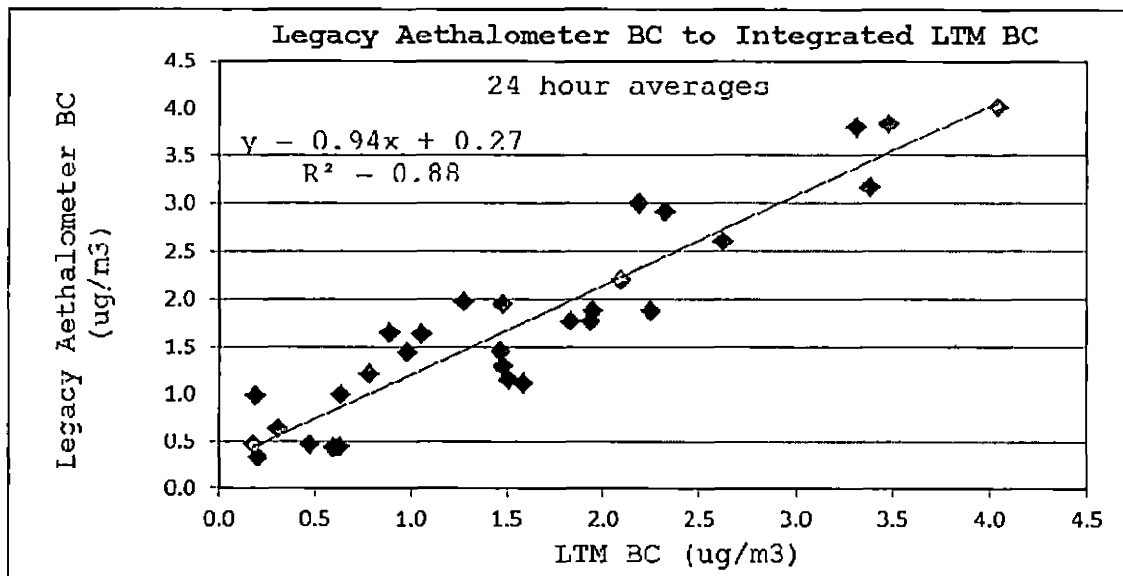


Figure 32. Legacy Aethalometers and Integrated Black Carbon

continuous BC and EC methods. The wavelength and geometry of the optics between the LTM BC and legacy aethalometers are similar. The two methods utilized different filter media with the LTM BC method using Teflon filters while the legacy aethalometers use a quartz fiber tape.

## CHAPTER FIVE

### SUMMARY AND CONCLUSIONS

An instrument comparison study was conducted to evaluate various BC and EC continuous and integrated measurement methods. This project provides a descriptive and comparative analysis of the data collected during an intensive field campaign conducted near the I-710 freeway from March 7 to April 8 of 2012. Previous works have attempted to characterize different methods for monitoring light absorbing aerosols, but the PAX, AE633 dual spot aethalometer, and the micro-aethalometers have never been compared prior to this study. The project is significant given the growing air quality concerns over the environmental and health effects of diesel PM and combustion particulates. A better understanding of the complexity of carbonaceous aerosols will help in developing control strategies, determining sources, refining air quality models, and understanding the effect of carbon on the environment and human health (Rice, 2004).

In this project, the observed BC and EC differences between methods has been reported. The effect of increasing averaging time on inter-method BC and EC correlations was



evaluated. As the averaging time increases, typically the  $R^2$  values get closer to one. Strong correlations were found for continuous BC and EC methods with  $R^2$  values always greater than 0.94 at the 1-hour averaging time for all continuous methods. The slope values between continuous instruments were found to vary from 0.74 to 1.52. Differences of a factor of 2 are common among other studies comparing methods for BC and EC concentrations (Watson et al., 2005). In this work, the averaged differences between the continuous BC and EC methods at the 1-hr time interval are less than a factor of 1.6 from one another. When comparing both continuous and non-continuous instruments, correlations at the 24-hour averaging time were also strong with  $R^2$  values always greater than 0.84. Slope values between methods ranged from 0.61 to 1.52 with an averaging time of 24-hour. Overall, the results of the inter-comparison including all the instruments show strong correlations among the methods with wide slope variations.

The fact that EC and BC measurements from such a wide variety of measurement techniques are highly correlated is significant, and the results of this thesis suggest that it may be possible to reconcile EC and BC measurements from optical, thermal-optical, and photoacoustic methods.

For 24-hour data, both the MAAP and AE633 are on average within 10% of the integrated thermal EC measurement. With the thermal EC as the x axis, the slope values would be 1.09 for the AE633 and 1.06 for the MAAP. The  $R^2$  value is greater than 0.93 for both of these continuous BC measurements when compared to the integrated thermal EC. Less than 8% of the variation in the BC measurements of these two methods is not explained by the variation in the integrated thermal EC measurement. The similarity of these results is striking when taking into account the drastic differences in methodology between continuous instruments and integrated filter analysis. The amount of time and resources needed to produce integrated filter EC results is significantly more than what is required to operate continuous BC monitors. Based on the results of this study, continuous measurements would be recommended over integrated filter measurements for measuring carbonaceous PM. Continuous instruments also provide time resolved data that may be beneficial or even necessary for source apportionments, refining air quality models, and understand effects of carbon on health and environment.

Various assumptions are used to convert an instrument signal into concentration; because of this, different methods produce different EC/BC results (slopes  $>$  or  $<$  than 1). With the strong correlations between these methods, the results indicate that these differences between methods are systematic and potentially reconcilable.

As this paper is primarily a descriptive/comparative analysis of the BC and EC data collected during this study, further investigation into the factors that are responsible for slope variability is recommended in order to better characterize the individual methods. Some of the potential causal factors for the differences between methods have been briefly discussed. Further investigation into the data set of this comparison study is required to understand the extent and causality of these factors in creating the differences between methods.

No suitable reference material for EC or BC is available to determine the precision and accuracy of the methods. Research into potential suitable reference materials for BC and EC is recommended. If such a reference material could be developed, the uncertainty of carbonaceous aerosol field measurements would be reduced.

The length of this comparison study was limited with an intensive sampling period spanning five weeks from March to April of 2012. Since, instrumental response may potentially be affected by seasonal variations in ambient temperature, atmospheric pressure, and other meteorological parameters, the comparison results between two methods may vary between different seasons. Future investigations should address potential seasonal differences between the various BC and EC measurements.

BC to EC differences may also be affected by the monitoring location, and the results of this study do not necessarily apply to geographical areas characterized by a different pollution source mix. However, the results of this study may be applicable to similar near roadway environments.

Additional work will be conducted to better characterize the effects of wind speed and direction, and traffic activity on the observed BC-EC differences.

Before recently developed BC and EC instruments can be utilized in routine monitoring networks, additional inter-comparison studies are needed to expand the objectives of this work.

## REFERENCES

- Ackerman, A.S.; Toon, O.B. Absorption of Visible Radiation in Atmosphere Containing Mixtures of Absorbing and Nonabsorbing Particles. *Appl. Opt.* **1981**, *20*, 3661-3667.
- Ahmed, T.; Dutkiewicz, V.; Shareef, A.; Tuncel, G.; Tuncel, S.; Husain, L. Measurement of Black Carbon (BC) by an Optical Method and a Thermal-optical Method: Inter-comparison for Four Sites. *Atmos. Environ.* **2009**, *43*, 6305-6311.
- Allen, G.; Lawrence, J.; Koutrakis, P. Field Validation of Semi-continuous Method for Aerosol Black Carbon (Aethalometer) and Temporal Patterns of Summertime Hourly Black Carbon Measurements in Southwestern PA. *Atmos. Environ.* **1999**, *33*, 817-823.
- Andreae, M.O.; Gelencsér, A. Black Carbon or Brown carbon? The Nature of Light-Absorbing Carbonaceous Aerosols. *Atmos. Chem. Phys.* **2006**, *6*, 3131-3148.
- Arnott, W.; Hamasha, K.; Moosmüller, H.; Sheridan, P.J.; Ogren J.A. Towards Aerosol Light-absorption Measurements with a 7-wavelength Aethalometer: Evaluation with a Photoacoustic Instrument and 3-

- wavelength Nephelometer. *Aerosol Sci. Technol.* **2005**, 39, 17-29.
- Arnot, W.; Moosmüller, H.; Sheridan, P.J.; Ogren, J.A.; Raspet, R.; Slaton, W.V.; Hand, J.L.; Kreidenweis, S.M.; Collett, J.L. Photoacoustic and Filter-based Ambient Aerosol Light Absorption Measurements: Instrument Comparison and the Role of Relative Humidity. *J. Geophys. Res.* **2003**, 108, 15-1 to 15-11.
- Bae, M.; Hong, C.; Kim, Y.; Han, J.; Moon, K.; Kondo, Y.; Komazaki, Y.; Miyazaki, Y. Intercomparison of two Different Thermal-optical Elemental Carbon and Optical Black Carbon during ABC-EAREX2005. *Atmos. Environ.* **2007**, 41(13), 2791-2803.
- Bae, M.; Lee, J.; Kim, Y.; Oak, M.; Shin, J.; Lee, K.; Lee, H.; Lee, S.; and Kim, Y. Analytical Methods of Levoglucosan, a Tracer for Cellulose in Biomass Burning, by Four Different Techniques. *Asian J. of Atmos. Environ.* **2012**, 6-1, 53-66.
- Bae, M.; Schauer, J.; DeMinter, J.; Turner, J.; Smith, D.; Cary, R. Validation of a Semi-continuous Instrument for Elemental Carbon and Organic Carbon using a Thermal-optical Method. *Atmos. Environ.* **2004**, 38(18), 2885-2893.

- Bae, M.; Schauer, J.; Turner, J.; Hopke, P. Seasonal Variations of Elemental Carbon in Urban Areas as Measured by two Common Thermal-optical Carbon Methods. *Sci. Total Environ.* **2009** *407*, 5176-5183.
- Birch, M.; Cary, R. Elemental Carbon-based Method for Monitoring Occupational Exposures to Particulate Diesel Exhaust. *Aerosol Sci. Technol.* **1996**, *25*, 221-241.
- Bond, T.C.; Sun, H.L. Can Reducing BC Emissions Counteract Global Warming? *Environ. Sci. & Technol.* **2005**, *39*, 5921- 5926.
- Caltrans: Performance Measurement System (PeMS).  
<http://pems.dot.ca.gov> (accessed May 11, 2012).
- Chameides, W.L.; Yu, H.; Liu, S.C.; Bergin, M.; Zhou, X.; Mearns, L.; Wang, G.; Kiang, C.S.; Saylor, R.D.; Luo, C.; Huang, Y.; Steiner, A.; Giorgi F. Case Study of the Effects of Atmospheric Aerosols and Regional Haze on Agriculture: An Opportunity to Enhance Crop Yields in China through Emission Controls. *Proc. Natl. Acad. Sci. USA* **1999**, *96*, 13626-13633.
- Chow, J.; Watson, J.; Chen, L.; Arnott, W.; Moosmuller, H. Equivalence of Elemental Carbon by Thermal/optical Reflectance and Transmittance with Different

- Temperature Protocols. *Environ. Sci. Technol.* **2004**, 38(16), 4414-4422.
- Chow, J.; Watson, J.; Crow, D.; Lowenthal, D.; Merrifield, T. Comparison of IMPROVE and NIOSH Carbon Measurements. *Aerosol Sci. and Technol.* **2001**, 34, 23-34.
- Chow, J.; Watson, J.; Doraiswamy, P.; Chen, L.; Sodeman, D.; Lowenthal, D.; Park, K.; Arnott, P.; Motallebi, N. Aerosol Light Absorption, Black Carbon, and Elemental Carbon at the Fresno Supersite, California. *Atmos. Res.* **2009**, 93(4), 874-887.
- Chow, J.; Watson, J.; Lowenthal, D.; Chen, L.; Motallebi, N. Black and Organic Carbon Emission Inventories: Review and Application to California. *J. Air Waste Manage. Assoc.* **2010**, 60(4), 497-507.
- Delfino, R.J.; Staimer, N.; Gillen, D.; Tjoa, T.; Sioutas, C.; Fung, K.; George, S.C.; Kleinman, M.T. Personal and Ambient Air Pollution is Associated with Increased Exhaled Nitric Oxide in Children with Asthma. *Environ. Health Perspect.* **2006**, 114, 1736-1743.
- Drinovec, L.; Močnik, G.; Zotter, P.; Prévôt, A.; Ruckstuhl, C.; Hansen, A. The "Dual-Spot" Aethalometer: Improved Measurement of Aerosol Black



Carbon with Real-time Loading Compensation. Presented at 2012 European Aerosol Conference. Grenada, Spain. <http://www.eac2012.com/EAC2012Book/files/692.pdf> (accessed on March 29, 2013).

Droplet Measurement Technologies (DMT). Photoacoustic Extinctionmeter (PAX). <http://www.dropletmeasurement.com/products/ground-based/pax.html> (accessed January 12, 2013).

Frank, N.; Rice, J.; Tikvart, J. Optical Measurements of CSN and FRM Teflon Filters to Estimate Elemental Carbon to Support Health Studies, PM NAAQS Implementation and Climate. Presented at National Air Monitoring Conference, Nashville, TN, November 4, 2009. Retrieved from [www.epa.gov/ttnamtl/files/2009conference/frankwed.pdf](http://www.epa.gov/ttnamtl/files/2009conference/frankwed.pdf)

Fruin, S.; Westerdahl, D.; Sax, T.; Sioutas, C.; Fine, P.M. Measurements and Predictors of On-road Ultrafine Particle Concentrations and Associated Pollutants in Los Angeles. *Atmos. Environ.* **2008**, *42*(2), 207-219.

Hansen, A. Magee Scientific. Personal Communication, 2013.

Hansen, A.; Rosen, H.; Novakov, T. The Aethalometer - An Instrument for the Real-time Measurement of Optical

- Absorption by Aerosol Particles. *Sci. Total Environ.* **1984**, *36*, 191-196.
- Jacobson, M. Strong Radiative Heating due to the Mixing State of Black Carbon in Atmospheric Aerosols. *Nature* **2001**, *409*, 695-697.
- Jacobson, M.; Hansson, H.; Noone, K.; Charlson, R. Organic Atmospheric Aerosols: Review and State of the Science. *Rev. Geophys.* **2000**, *38*(2), 267-294.
- Jeong, C.; Hopke, P.; Kim, E.; Lee, D. The Comparison between Thermal-optical Transmittance Elemental Carbon and Aethalometer Black Carbon Measured at Multiple Monitoring Sites. *Atmos. Environ.* **2004**, *38*(31), 5193-5204.
- Jernigan, J.; Goohs, K. Installation of the Model 5012 Multi-Angle Absorption Photometer for Real-time Black Carbon Monitoring. Presented at National Air Monitoring Conference [Online], Las Vegas, NV, November 6, 2006. <http://www.epa.gov/ttnamtl1/files/2006conference/goohs.pdf> (accessed Jan 14,2013).
- Kim, J.J.; Smorodinsky, S.; Lipsett, M.; Singer, B.C.; Hodgson, A.T.; Ostro, B. Traffic-related Air Pollution near Busy Roads: The East Bay Children's Respiratory

- Health Study. *Am. J. Respir. Crit. Care Med.* **2004**, *170*, 520-526.
- Kozawa, K.H.; Fruin, S.A.; Winer, A.M. Near-road Air Pollution Impacts of Goods Movement in Communities adjacent to the Ports of Los Angeles and Long Beach. *Atmos. Environ.* **2009**, *43*(18), 2960-2970.
- Lioussse, C.; Cachier, H.; Jennings, S. G. Optical and Thermal Measurement Methods of Black Carbon Aerosol Content in Different Environments: Variation of the Specific Attenuation Cross-Section, Sigma ( $\sigma$ ). *Atmos. Environ.* **1993**, *27*(8), 1203-1211.
- Mader, B.; Schauer, J.; Seinfeld, J.; Flagan, R.; Yu, J.; Yang, H.; Lim, H.; Turpin, B.; Deminter, J.; Heidemann, G.; Bae, M.; Quinn, P.; Bates, T.; Eatough, D.; Huebert, B.; Bertram, T.; Howell, S. Sampling Methods used for the Collection of Particle-phase Organic and Elemental Carbon during ACEAsia. *Atmos. Environ.* **2003**, *37*, 1435-1449.
- Magee Scientific: Air Sampling Products.  
[http://www.mageesci.com/air\\_sampling\\_products.html](http://www.mageesci.com/air_sampling_products.html)  
(accessed Jan 7, 2013)
- Multiple Air Toxics Exposure Study (MATES) III; South Coast Air Quality Management District: Diamond Bar, CA

<http://www.aqmd.gov/prdas/matesIII/MATESIIDraftFinalReportJuly2008.html> (accessed Jan 7, 2013)

National Ambient Air Quality Standards (NAAQS). United States Environmental Protection Agency.

<http://www.epa.gov/air/criteria.html> (accessed April 6, 2013)

National Institute for Occupational Safety and Health (NIOSH) 1996. Elemental Carbon (Diesel Particulate): Method 5040. In: Eller, P.M., Cassinelli, M.E. (Eds.), *NIOSH Manual of Analytical Methods*, fourth ed., Cincinnati.

Ostro, B.; Roth, L.; Malig, B.; Marty, M. The Effects of Fine Particle Components on Respiratory Hospital Admission in Children. *Environ. Health Perspect.* **2009**, *117*, 475-480.

Pandis, S.N.; Harley, R.A.; Cass, G.R.; Seinfeld, J.H. Secondary Organic Aerosol Formation and Transport. *Atmos. Environ.* **1992**, *26A*, 2269-2282.

Park, K.; Chow, J.; Watson, J.; Trimble, D.; Doraiswamy, P.; Arnott, Pat; Stroud, Kenneth; Bowers, Kenneth; Bode, Richard; Petzold, Andre; Hansen, A. D. Comparison of Continuous and Filter-based Carbon

- Measurements at the Fresno Supersite. *J. Air Waste Manage. Assoc.* **2006**, 56(4), 474-491.
- Park, S.; Hansen, A.; Cho, S. Measurement of Real Time Black Carbon for Investigating Spot Loading Effects of Aethalometer Data. *Atmos. Environ.* **2010**, 44(11), 1449-1455.
- Petzold, A.; Kopp, C.; Niessner, R. The Dependence of the Specific Attenuation Cross-Section on Black Carbon Mass Fraction and Particle Size. *Atmos. Environ.* **1997**, 31(5), 661-672.
- Petzold, A.; Kramer, H.; Schonlinner, M. Continuous Measurement of Black Carbon using a Multi-angle Absorption Photometer. *Environ. Sci. Pollut. Res.* **2002**, 4, 78-82.
- Petzold, A.; Schloesser, H.; Sheridan, P.; Arnott, P.; Ogren, J.; Virkkula, A. Evaluation of Multiangle Absorption Photometry for Measuring Aerosol Light Absorption. *Aerosol Sci. Technol.* **2005**, 39(1), 40-51.
- Rice, J. Comparison of Integrated Filter and Automated Carbon Aerosol Measurements at Research Triangle Park, North Carolina. *Aerosol Sci. Technol.* **2004**, 38, 23-36.
- Sasser, S.; Hemby, J.; Adler, K.; Anenberg, S.; Bailey, C.; Brockman, L.; Chappell L.; DeAngelo, B.; Damberg, R.;

- Dawson, J.; et al. *Report to Congress on Black Carbon*; United States Environmental Protection Agency: March 2012. <http://www.epa.gov/blackcarbon>. (accessed Jan 15, 2013)
- Schauer, J.; Mader, B.; Deminter, J.; Heidemann, G.; Bae, M.; Seinfeld, J.; Flagan, R.; Cary, R.; Smith, D.; Huebert, B.; Bertram, T.; Howell, S.; Kline, J.; Quinn, P.; Bates, T.; Turpin, B.; Lim, H.; Yu, J.; Yang, H.; Keywood, M. ACE-Asia Intercomparison of a Thermal-optical Method for the Determination of Particle-phase Organic and Elemental Carbon. *Environ. Sci. Technol.* **2003**, 37, 993-1001.
- Seinfeld, J.; Pandis, S. *Atmospheric Chemistry and Physics: From Air Pollution to Climate Change*. New York: Wiley. Wiley-Interscience; 1 edition 1997 (November 6, 1997)
- Sheridan, P.; Arnott, W.; Ogren, J.; Andrews, E.; Atkinson, Dean; Covert, David; Moosmuller, Hans; Petzold, Andreas; Schmid, Beat; Strawa, Anthony; Varma, Ravi; Virkkula, Aki. The Reno Aerosol Optics Study: An Evaluation of Aerosol Absorption Measurement Methods. *Aerosol Sci. Technol.* **2005**, 39(1), 1-16.
- Snyder, D.; Schauer, J. An Inter-comparison of two Black Carbon Aerosol Instruments and a Semi-continuous

- Elemental Carbon Instrument in the Urban Environment. *Aerosol Sci. Technol.* **2007**, *41*(5), 463-474.
- Sunset Laboratory. <http://www.sunlab.com/products-services/model-4-field-analyzer.html> (accessed Jan 7, 2013).
- Tolocka, M.; Solomon, P.; Mitchel, W.; Norris, G.; Gemmill, D.; Weiner, R.; Vanderpool, R.; Homolya, J.; Rice, J. East verses West in the US: Chemical Characteristics of PM<sub>2.5</sub> during Winter of 1999. *Aerosol Sci. Technol.* **2001**, *34*(1), 88-96.
- Turpin, B.J.; Huntzicker, J.J.; Hering, S.V. Investigation of Organic Aerosol Sampling Artifacts in the Los Angeles Basin. *Atmos. Environ.* **1994**, *28*(19), 3061-3071.
- U.S. Environmental Protection Agency (USEPA). (2002). Latest Findings on National Air Quality: 2001 Status and Trends. EPA 454/K-02-001, USEPA, Office of Air Quality Planning and Standards, Research Triangle Park, NC, September 2002. Retrieved from <http://www.epa.gov/air/aqtrnd01/>
- Watson, J. Visibility: Science and Regulation. *J. Air Waste Manage. Assoc.* **2002**, *52*(6), 628-713.

- Watson, J.; Chow, J. Comparison and Evaluation of In-situ and Filter Carbon Measurements at the Fresno Supersite. *J. of Geophys. Res.* **2002**, 107, 3-15.
- Watson, J.; Chow J.; Chen, A. Summary of Organic and Elemental Carbon/Black Carbon Analysis Methods and Intercomparisons. *Aerosol and Air Quality Res.* **2005**, 5(1), 65-102.
- Weather Underground: History for Long Beach, CA.  
[http://www.wunderground.com/history/airport/KLGB/2012/3/7/CustomHistory.html?dayend=8&monthend=4&yearend=2012&req\\_city=NA&req\\_state=NA&req\\_statename=NA&MR=1](http://www.wunderground.com/history/airport/KLGB/2012/3/7/CustomHistory.html?dayend=8&monthend=4&yearend=2012&req_city=NA&req_state=NA&req_statename=NA&MR=1)  
(accessed April 12, 2013).
- Weingartner, E.; Saathoff, H.; Schnaiter, M.; Streit, N.; Bitnar, B.; Baltensperger, U. Absorption of Light by Soot Particles: Determination of the Absorption Coefficient by Means of Aethalometers. *J. Aerosol Sci.* **2003**, 34, 1445-1463.
- Yang, M.; Howell, S. G.; Zhuang, J.; Huebert, B. J. Attribution of Aerosol Light Absorption to Black Carbon, Brown Carbon, and Dust in China - Interpretations of Atmospheric Measurements during EAST-AIRE. *Atmos. Chem. Phys.* **2009**, 9, 2035-2050.



Zhu, Y.; Hinds, W.; Kim, S.; Shen, S.; Sioutas, C. Study of Ultrafine Particles near a Major Highway with Heavy-duty Diesel Traffic. *Atmos. Environ.* **2002a**, 36, 4323-4335.

Zhu, Y.; Hinds, W.; Kim, S.; Sioutas, C. Concentration and Size Distribution of Ultrafine Particles near a Major Highway. *J. Air Waste Manage. Assoc.* **2002b**, 52(9), 1-2.